Deep–Sea Research II 208 (2023) 105267

Contents lists available at ScienceDirect

Deep-Sea Research Part II

journal homepage: www.elsevier.com/locate/dsr2

New and known species of the genus *Desmodora* De Man, 1889 (Nematoda: Desmodoridae) from the hydrothermal vent communities of the Piip volcano (south-west Bering Sea)

V.V. Mordukhovich [a,b], N.P. Fadeeva [a,*], A.A. Semenchenko [a,c], S.I. Kiyashko [b], E.R. Scripova [a]

[a] Far Eastern Federal University, Vladivostok, 690922, Russia
[b] A.V. Zhirmunsky National Scientific Center of Marine Biology, Far Eastern Branch, Russian Academy of Sciences, Vladivostok, 690041, Russia
[c] Federal Scientific Center of the East Asia Terrestrial Biodiversity, Far Eastern Branch, Russian Academy of Sciences, Vladivostok, 690022, Russia

ARTICLE INFO

Handling Editor: Prof. J Aristegui

Keywords:
Deep-sea communities
Marine nematodes
Integrative taxonomy
Spatial distribution
Trophic ecology
Biomarkers
Fatty acids
Stable isotopes

ABSTRACT

Species of the marine nematode of the genus *Desmodora* have been found to dominate (up to 78%) in the nematode fauna from the hydrothermal vent communities of submarine Piip volcano, Bering Sea. The morphological characteristics and molecular genetic data of *Desmodora* specimens from different habitats of the volcano were studied and three new and one known species have been described: *Desmodora hydrothermica* sp. nov., *Desmodora marci, Desmodora spongiophila* sp.nov., *Desmodora spongiocola* sp.nov. The species often lived together, but a pronounced spatial specialization was observed. *Desmodora spongiophila* sp.nov. and *Desmodora spongiocola* sp.nov. were abundant inhabitants of the vulcanellids and some hexactenellids. *Desmodora hydrothermica* sp.nov. dominated in microbial mats on the carbonate chimneys from the South Summit, while *Desmodora marci* was found on stones near vents and in bottom sediments with *Calyptogena pacifica* (Bivalvia: Vesicomyidae). The last two species were already known in deep-sea reduced environments of the Pacific and Atlantic oceans, in similar habitats. The $\delta^{13}C$ and $\delta^{15}N$ values and fatty acids composition of *Desmodora* samples from hydrothermal habitats confirmed the consumption of chemosynthetically derived organic matter. SSU and D2-D3 of LSU phylogenetic trees largely agree with those of previous analyses indicating that *Desmodora* is not monophyletic. Moreover, phylogenetic relationships within the subfamily Desmodorinae remained unresolved.

1. Introduction

Currently, there is an increasing interest in the study of benthic animals inhabiting deep-sea reducing environments such as hydrothermal vents and methane seeps. Such environments are widespread in the World Ocean and their study allows us to expand our understanding of the formation, composition, structure, functioning of marine ecosystems, in particular, in extreme habitat conditions. (Danovaro et al., 2017; Dodd et al., 2017; German et al., 2011; Levin et al., 2016; Nisbet and Sleep, 2001). The usual inhabitants of such communities are free-living nematodes, often characterized here by a very high abundance (Zeppilli and Leduc, 2018). It has been shown that nematodes are actively involved in the transformation of organic matter of chemosynthetic origin (Van Gaever et al., 2009; Van Campenhout and Vanreusel, 2016). However, the quantitative assessment of the role of nematodes in the fluxes of matter and energy is still complicated by the paucity of data on their trophic ecology.

Studies of the taxonomic composition of meiofauna associated with deep-sea chemosynthetic environments in the Pacific ocean are confined mainly to a small number of areas, in particular, East Pacific Rise (for example, Dinet et al., 1988; Flint et al., 2006; Zekely et al., 2006a,c; Copley et al., 2007; Gollner et al., 2013, 2015a, b, 2020), Lau Basin (Decraemer and Gourbault 1997; Verschelde et al., 1998; Diaz-Recio Lorenzo et al., 2021), Izu-Ogasawara Arc (Uejima et al., 2017; Senokuchi et al., 2018; Nomaki et al., 2019; Nakasugi et al., 2021). Studies of the deep-sea meiofauna of hydrothermal vents and cold seeps in the North-Western Pacific are very scarce (Shirayama, 1992; Shirayama and Ohta, 1990; Setoguchi et al., 2014; Nakasugi et al., 2021; Watanabe et al., 2021) and none provides information about the species composition of the nematofauna, the trophic relationships of nematodes, and the features of their distribution.

In general, data on the species composition of nematofauna from

* Corresponding author.
E-mail address: fadeeva.np@dvfu.ru (N.P. Fadeeva).

https://doi.org/10.1016/j.dsr2.2023.105267
Received 13 August 2022; Received in revised form 23 December 2022; Accepted 15 January 2023
Available online 26 January 2023

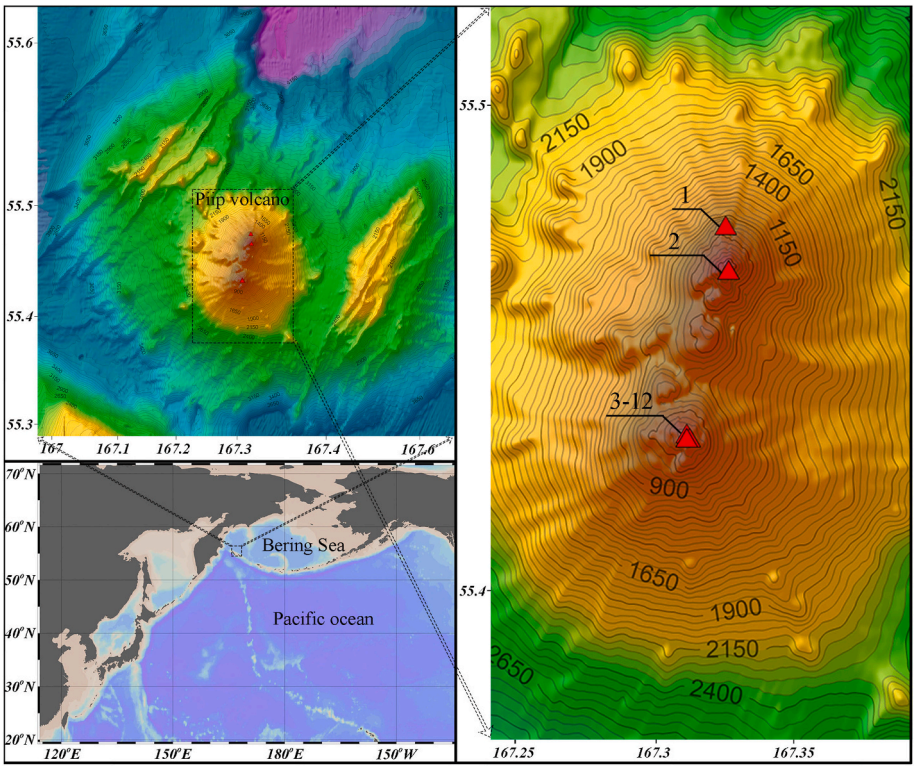

Fig. 1. Map showing the study station locations. 1 – North slope; 2 –North summit; 3–12 – South summit.

communities of the Pacific hydrotherms are limited to descriptions of a few dominant species: *Dinetia nycterobia* from the East Pacific Rise and *Cephalochaetosoma pacificum notium* from Lau-Fidji Bassin (Decraemer and Gourbault, 1997); *Halomonhystera fisheri* and *H. hickei* from East Pacific Rise (Zekely et al., 2006b); *Linhomoeus caudipapillosus* and *Neochromadora* aff. *poecilosoma* – East Pacific Rise (Gollner et al., 2013); *Desmodora alberti*, *Desmodorella balteata*, *Desmodorella spineacaudata* – East Pacific Rise, *Desmodora marci* – Lau Basin (Verschelde et al., 1998).

Analysis of available data on spatial distribution free-living nematodes associated with chemosynthetic environments in the deep sea, showed a high taxonomic similarity of communities (at the level of genera) in the fields of fluid emissions and adjacent areas, there is no unique affinity of particular nematode taxa with seeps or vents (Vanreusel et al., 2010).

However, the lack of detailed information on the nematofauna of deep-sea hydrotherms does not allow generalizations about the uniqueness of the fauna and patterns of distribution at the species level. A number of species show obvious confinement to the hydrotherms and seeps. In particular, *Desmodora marci*, in addition to the hydrothermal vents in the Lau Basin in the South-West Pacific, was found on carbonate rocks and sulphide-oxidizing bacterial mats at Hydrate Ridge methane seeps (off the coast of Oregon, North-East Pacific) (Sapir et al., 2014) and in hydrothermal sites of the North Mid-Atlantic Ridge (Tchesunov, 2015).

During the 75th (2016) and 82nd (2018) cruises of the RV *Akademik M.A. Lavrentyev* (Galkin and Ivin, 2019; Galkin et al., 2019) samples were taken for the first time for the study of nematofauna from hydrothermal sites of submarine Piip Volcano (the southwestern Bering Sea) – the northernmost hydrothermal region in the Pacific. Preliminary studies have revealed a significant diversity and abundance of desmodorid nematodes, their relative abundance reached 78% in some habitats.

The aims of the present contribution are taxonomic descriptions of *Desmodora* species from hydrothermal sites of submarine Piip Volcano, studying the features of their distribution and trophic ecology.

2. Material and methods

2.1. Study area and sampling

A total of 25 samples were collected in 2016 and 2018 at the summits of Piip submarine volcano (the Volcanologists Massif, Bering Sea) during the 75th and 82nd research cruises aboard the R/V *Akademik Lavrentiev*. The Piip Volcano constitutes the central part of the Volcanologists Massif situated between the Alpha Ridge and the Bering Fracture Zone in the southern part of the Komandorsky Basin (Baranov et al., 1991, 2021). Hydrothermal vents were found on the Northern and Southern summits of the volcano, the distance between summits is about 4 km (Baranov et al., 2021). Most of the hydrothermal manifestations were confined to the depths from ~368 to 421 m and from ~464 to 495 m on the Northern and Southern summits, respectively. For more detailed information on the environmental parameters and communities see Seliverstov (2009), Galkin et al. (2019), Polonik (2018), and Rybakova et al. (2023).

The samples were collected using ROV *Comanche-18* (Sub-Atlantic, UK) by the mechanical arm or nets with a metal square frame (15 × 15 cm) equipped with a double bag (Figs. 1 and 2; Table 1). Photo and video footage were collected during the ROV dives. On deck, about 1 L of the bottom sediment from the net was carefully sieved through 1000, 500 and 32 μm mesh sizes. The hydrothermal chimneys were gently rinsed with cold filtered seawater and the bacterial mats were brushed off with a soft brush and then washout was bolted through 32 μm mesh sizes. The sponges were kept for several hours in chilled filtered sea water, then rinsed five times and washout was bolted through 32 μm mesh sizes. In all cases one-third of the sample was fixed with 4% buffered formaldehyde, one-third was fixed with DESS (solution of 0.25 M disodium EDTA and 20% dimethyl sulphoxide (DMSO), saturated with NaCl, pH 8.0) and then was stored in the laboratory at 4 °C, and one-third of the sample was frozen (−20 °C). Additional samples of bacterial mats and bottom sediments were oven-dried at 60 °C for 48 h and stored in the desiccator for stable isotopes analyses.

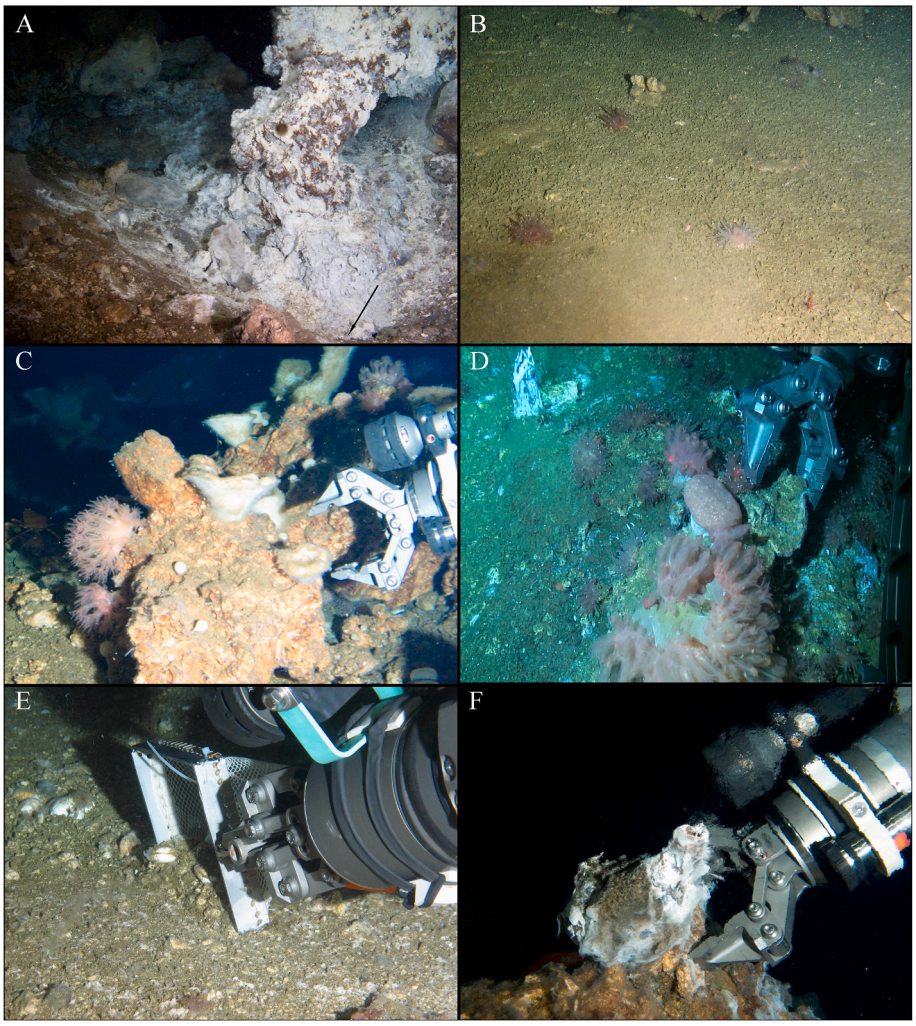

Fig. 2. Studied habitats. A – station 2, anhydrite structures, the arrow indicates the sampling site; B – station 7, outside hydrothermal fields; C – station 3, *Vulcanella*; D – station 4, stones in the vicinity of the vent; E – station 6, bottom sediments with *Calyptogena pacifica*; F – station 9, hydrothermal chimney.

2.2. Microscopy

In the laboratory, fixed samples were sorted using stereomicroscopes. For the optical microscopy 150 individuals of nematodes were picked out and transferred to glycerine using the Seinhorst's (1959) rapid method as modified by De Grisse (1969) and mounted on permanent slides. Drawings and DIC (differential interference contrast) photographs were made on an optical microscope Olympus BX 53 with the aid of a drawing tube and a digital camera respectively.

For the scanning electron microscopy, specimens were gradually dehydrated in a series of baths of increasing ethanol content, dried in a critical-point dryer, sputter-coated with gold and observed and imaged with a Zeiss Sigma 300 VP scanning electron microscope (SEM).

The type material is deposited at MIMB, the Museum of the A.V. Zhirmunsky National Scientific Center of Marine Biology FEB RAS (NSCMB FEB RAS), formerly Institute of Marine Biology FEB RAS, Vladivostok, Russia.

Abbreviations related to measurements presented in the descriptions are.

a – body length divided by maximum body diameter;
b – body length divided by esophageal length;
c' – tail length divided by cloacal/anal body width;
c – body length divided by tail length;
cbd. – corresponding body diameter;
L – body length, (μm);
V (%) – distance of vulva from the anterior end as a percentage of body length, (%).

2.3. Molecular analyses

For molecular analyses, specimens of *Desmodora* were picked out from the DESS samples under a stereoscopic microscope, mounted on temporary slides with sterile distilled water and observed at different magnifications using a light microscope (Olympus BX 53) with differential interference contrast, and equipped with a digital camera. Specimens were identified and photographed (the entire habitus, head, midbody, and tail region). After the photo-vouchering, total DNA was extracted from the whole body of adult nematodes using the Qiagen DNeasy extraction kit according to the protocol. Fragments of the short and long subunits of nuclear ribosomal DNA were PCR amplified. For 18S rDNA, we used the primer set SSU_F_03 (f): 5′-GCT TGT CTC AAA GAT TAA GCC ATG C-3' (Blaxter et al., 1998) and SSU_R_81 (r): 5′-GTA TCT GAT CGC CKT CGA WC-3' (Blaxter et al., 1998) which amplifies a fragment of ca 1800 bp. We use additional primers to sequence 18S rDNA amplicons: SSU_F_24_1 (f): 5′-AGA GGT GAA ATT CTT GGA TC-3' (Meldal et al., 2007) and MN18R (r) 5′- GGG CGG TAT CTG ATC GCC-3' (Floyd et al., 2005). The D2-D3 region of the 28S ribosomal DNA region was amplified using the primers D2a (f): 5′-ACA AGT ACC GTG AGG GAA AGT TG-3′ and D3b (r): 5′-TCG GAA GGA ACC AGC TAC TA-3'

Table 1
Study site and sampling details.

N	Depth [m]	Date dd/mm/yy	Latitude	Longitude	Area	Habitat	Collecting tool	*Desmodora* species
1	783	19.06.2016	55.425	167.275	North slope	Hexactinellida	Mechanical arm	*D. spongiophila* sp.nov.
2	395	13.06.2016	55.416	167.276	North Summit	Anhydrite structures	Net	*D. spongiophila* sp.nov.
3	472	23.06.2016	55.383	167.261	South Summit	Demospongiae: *Vulcanella*	Mechanical arm	*D. spongiophila* sp.nov.
4	466	26.06.2016	55.382	167.261	South Summit	Stones in the vicinity of the vent	Mechanical arm	*D. hydrothermica* sp.nov., *D. marci*, *D. spongiophila* sp.nov., *D. spongiocola* sp. nov.
5	468	26.06.2016	55.382	167.261	South Summit	Hydrothermal chimney	Mechanical arm	*D. hydrothermica* sp.nov.
6	469	26.06.2016, 17.06.2018	55.382	167.262	South Summit	Bottom sediments with *Calyptogena pacifica* (sand, gravel)	Net	*D. hydrothermica* sp.nov., *D. marci*, *D. spongiocola* sp.nov.
7	470	17.06.2018	55.382	167.261	South Summit	Bottom sediments outside hydrothermal fields (sand, gravel	Net	*Desmodora* species not found
8	468	26.06.2016	55.382	167.262	South Summit	Demospongiae: *Vulcanella*	Mechanical arm	*D. spongiophila* sp.nov., . *spongiocola* sp.nov.
9	452	26.06.2016	55.382	167.261	South Summit	Hydrothermal chimney	Mechanical arm	*D. hydrothermica* sp.nov.
10	382	13.06.2018	55.416	167.276	North Summit	Demospongiae: *Poecillastra*	Mechanical arm	*D. spongiophila* sp.nov.
11	469	14.06.2018	55.382	167.261	South Summit	Demospongiae: *Vulcanella*	Mechanical arm	*D. spongiocola* sp.nov.
12	458	17.06.2018	55.382	167.261	South Summit	Hydrothermal chimney	Mechanical arm	*D. hydrothermica* sp.nov.

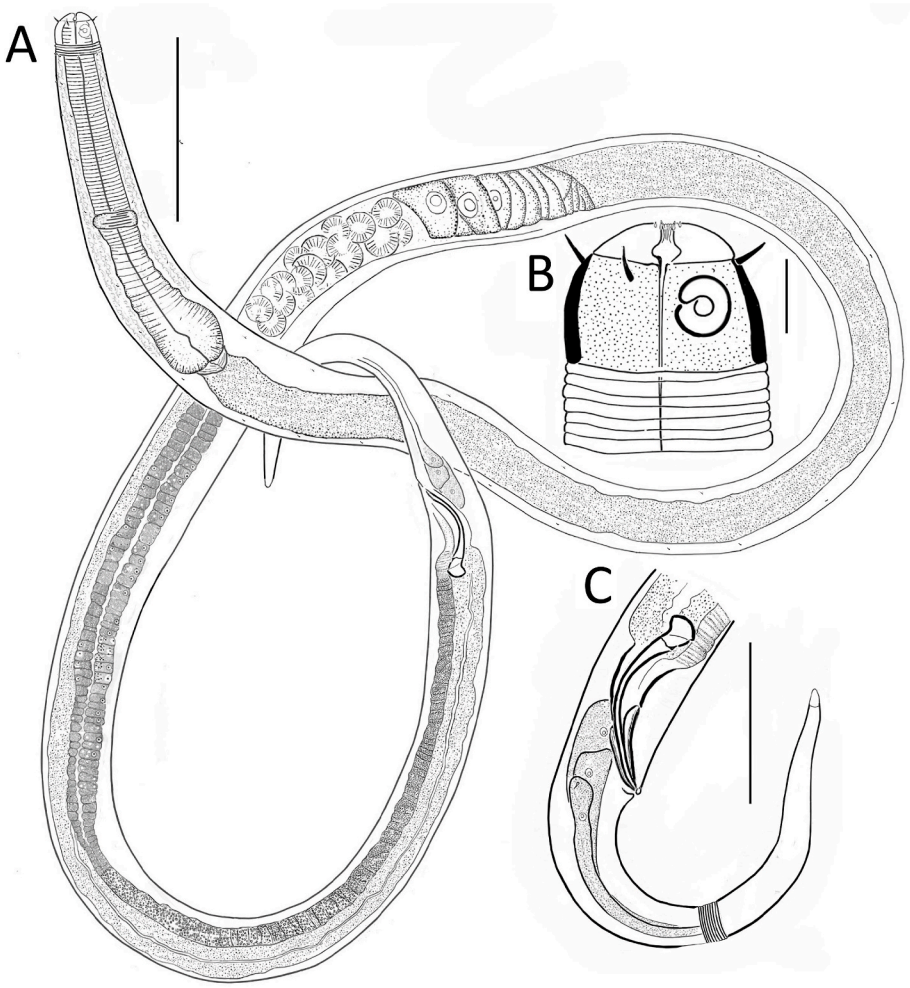

Fig. 3. *Desmodora hydrothermica* sp. nov. Male. A. General view. B. Cephalic region. C. Tail. Scale bars: A – 100 μm, B – 10 μm, C – 50 μm.

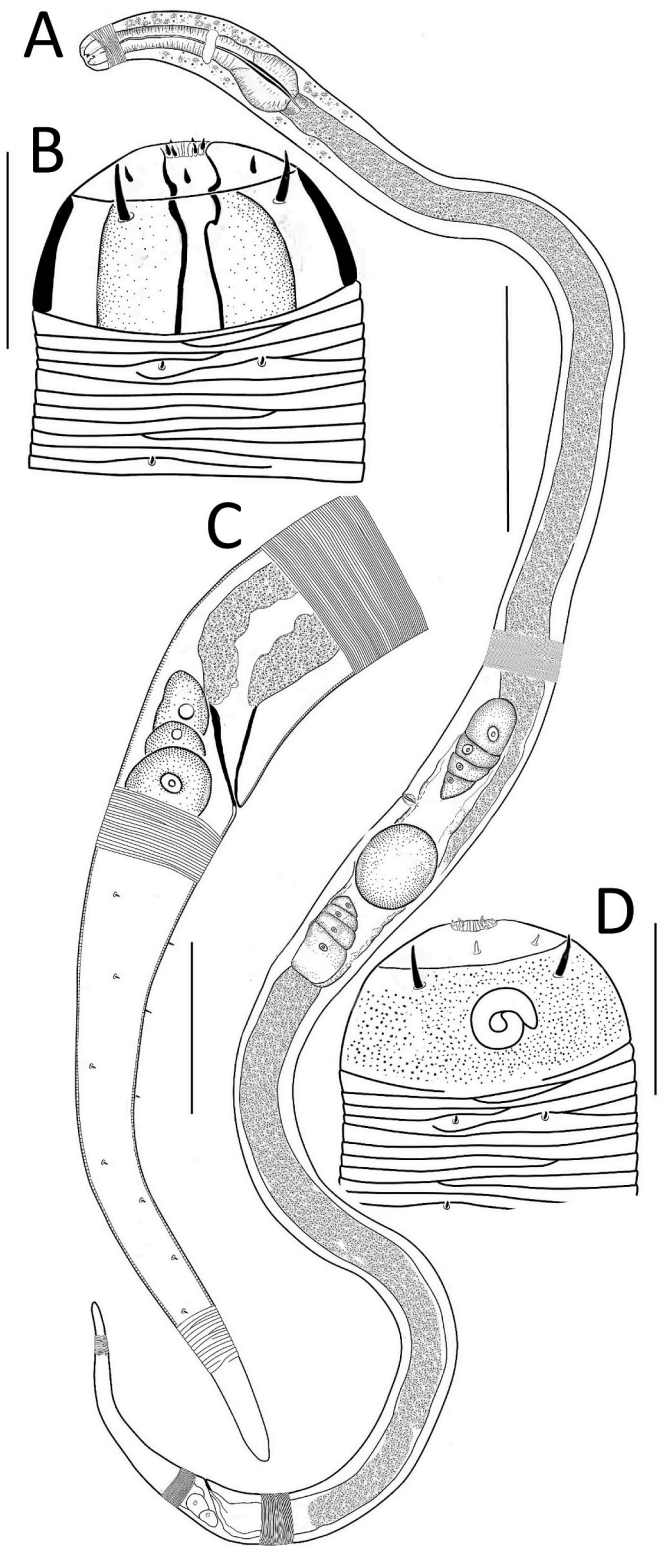

Fig. 4. *Desmodora hydrothermica* sp. nov. Female. A. General view. B, D. Cephalic region. C. Tail. Scale bars: A. – 200 μm; B, D – 20 μm; C – 50 μm.

(Nunn, 1992). The length of the obtained amplicon was 700 bp.

PCR reactions for obtained amplicons were run in a total volume of 10 μl with 5 μl Go Taq Green Master Mix (Promega corp, Madison, WI, USA), 0.5 μM of each primer, 3 μl nuclease-free water and 1 μl of genomic DNA. The PCR thermal regime consisted of one cycle of 1 min at 94 °C; 35 cycles of 30 s at 94 °C, 30 s at 56 °C and 1–2 min at 72 °C and a final cycle of 5 min at 72 °C. Each PCR fragment was purified using Exonuclease I (ExoI) and Thermosensitive Alkaline Phosphatase (FastAP) (Thermo Fisher Scientific Inc., USA). Sequencing reactions had a total volume of 10 μl and included 10 pmol of each primer and reagents of BigDye terminator v3.1 cycle kit. The sequencing amplification protocol consisted of one cycle of 1 min at 98 °C, followed by 30 cycles of 10 s at 96 °C, 5 s at 50 °C, and 4 min at 60 °C. The PCR products were bidirectionally sequenced using the BigDye Terminator v3.1 cycle kit and run on an ABI 3130xl (Applied Biosystems™). Sequences were manually assembled and edited using Finch TV and MEGA 7 (Kumar et al., 2016).

The obtained sequences were checked and aligned at the nucleotide level using T-Coffee algorithm (Magis et al., 2014) on a MPI Bioinformatics Toolkit web service (Zimmermann et al., 2018). Bayesian phylogenetic analyses were conducted with MrBayes v. 3.2.7a (Ronquist et al., 2012). For tree reconstruction, we used the obtained sequences, as well as dataset from GenBank belonging to families Desmodoridae and Monoposthiidae (order Desmodorida), with length more than 1000 bp for 18S and 650 bp for D2-D3 region 28S rDNA. PartitionFinder 2.1.1 (Lanfear et al., 2012) was used to select the best-fit partitioning scheme and models for each ribosomal loci using the greedy algorithm with linked branch lengths for the corrected Akaike Information Criterion as the optimality criterion for model selection. The best models for both ribosomal loci were GTR + I + G. Bayesian Inference was performed with two independent runs of Metropolis-coupled Markov chain Monte Carlo analyses, with each run comprising one cold chain and three heated chains at a default temperature of 0.1. The chains were run for 10 million generations and sampled every 100 generations. A burn-in of 2.5 million generations (or 25% of the sampled trees) was used. Moreover, trace files were visually inspected in Tracer 1.7 (Rambaut et al., 2018). RAxML v. 8.2.4 (Stamatakis, 2006) was used to conduct a maximum likelihood (ML) and bootstrap analysis (1000 replications) using the GTR plus G model. FigTree v. 1.4.4 was used to visualize phylogenetic trees after analysis.

2.4. Stable isotope analysis

Each sample of washout was unfrozen, and nematodes were picked out with a fine needle under a stereomicroscope. The specimens were rinsed twice with distilled water to remove any adhered particles and transferred to a drop of distilled water in 5 × 9 mm tin cups (Euro-Vector). Tin cups containing nematodes were oven-dried at 60 °C for 24 h, sealed and stored in screw-cap glass tubes until analysis; the samples were not acidified. Samples for analyses consisted of 6–150 individuals (Table 4).

Oven-dried samples of bacterial mat were ground to a homogeneous fine powder using an agate mortar and pestle, and the 0.5 mg subsamples were packaged into tin caps. Samples of bottom sediments were ground with a mortar and pestle and two subsamples (each ~500 mg dry weight) were prepared for $\delta^{13}C$ and $\delta^{15}N$ measurements. The subsamples employed for $\delta^{13}C$ analysis were acidified with 1M HCl drop by drop until the effervescence ceased and was dried at 50 °C under a fume extractor to evaporate the acid. To prevent the loss of dissolved organic matter, acidified samples were not rinsed (Jaschinski et al., 2008).

All stable isotope analyses were performed at the Stable Isotope Laboratory (Far Eastern Geological Institute FEB RAS, Vladivostok) using a FlashEA 1112 elemental analyser coupled to a MAT 253 isotope mass spectrometer (ThermoQuest, Germany) by a ConFlo IV interface. Sample isotopic ratios were expressed in the conventional δ notation as parts per thousand (‰) according to the following equation:

$$\delta^{13}C \text{ or } \delta^{15}N = [(R_{sample} - R_{standard})/ R_{standard}] \text{ x } 1000$$

where $R = {}^{13}C/{}^{12}C$ or ${}^{15}N/{}^{14}N$. The δ values were expressed relative to the international reference standards of Pee Dee Belemnite for carbon and atmospheric N_2 for nitrogen. The internal laboratory standard was

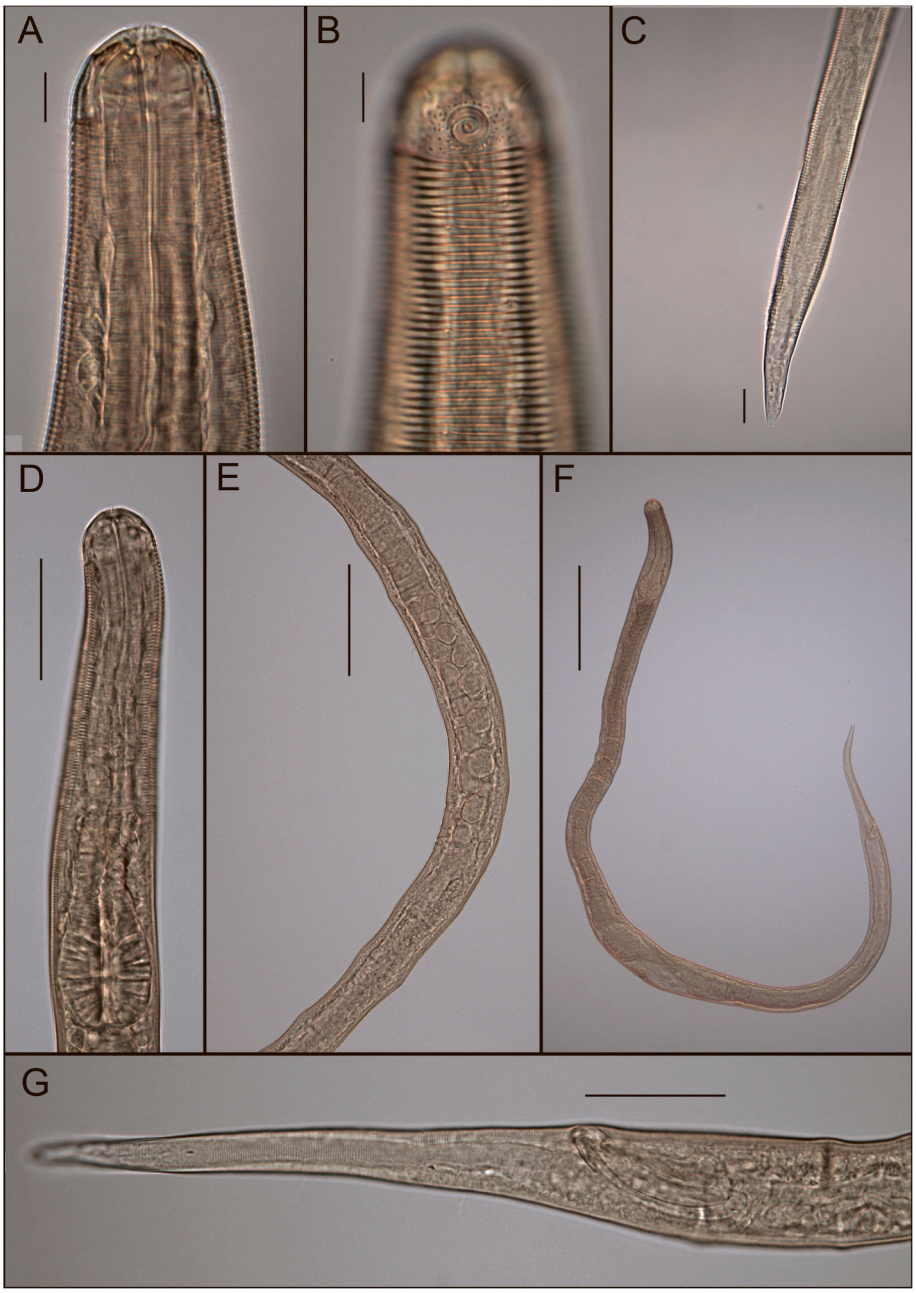

Fig. 5. *Desmodora hydrothermica* sp. nov. Light microscopy, DIC. A-B. Male cephalic region. C. Tail tip. D. Anterior region of male. E. Testis. F. Female body. G. Male tail. Scale bars: A, B, C – 10 μm; E – 100 μm; F – 200 μm; D, G – 50 μm.

measured after every sixth sample during analysis for data quality control purposes. Based on the SD of the replicates of the laboratory standard, the internal precision was ±0.1‰ for both $\delta^{13}C$ and $\delta^{15}N$.

Significance of differences in stable isotope signatures were tested by *t*-test. The analyses were performed using Past 4.09 (Hammer et al., 2001). A statistical probability of $p < 0.05$ was considered significant.

2.5. Fatty acids analysis

Samples were unfrozen and specimens of *Desmodora hydrothermica* sp. nov. (500 individuals for each replicate) were picked out with a fine needle under a stereomicroscope. The specimens were rinsed twice with distilled water to remove any adhered particles and placed in vials containing a chloroform-methanol mixture (1:1, v/v). Sorting was restricted to individuals of *Desmodora hydrothermica* sp. nov. since they were easily recognizable under a stereomicroscope by general habitus and body size and were available in a sufficient biomass.

Lipids were extracted from all samples using the extraction method of Bligh and Dyer (1959). Fatty acid methyl esters (FAMEs) were prepared from the total lipids according to the procedure by Carreau and Dubacq (1978) and purified with preparative thin layer chromatography in benzene. The 4.4-dimethyloxazoline derivatives of FAs were prepared according to Svetashev (2011). FAMEs were analysed on a Shimadzu GC 2010 chromatograph using a fused quartz capillary (30 m × 0.25 mm) column coated with SUPELCOWAX 10 (Supelco). FAs were identified based on the gas chromatography-mass spectrometry data from the FAMEs and from the 4,4-dimethyloxazoline derivatives of the FAs. Mass spectrometry was performed on a Shimadzu GCMS QP5050A spectrometer using MDN 5S columns (temperature gradient from 170 °C to 290 °C at 2 °C min^{-1} and then held for 25 min). All spectra were obtained using the electron impact method at 70 eV, and the spectra were compared with the NIST library and an online FA mass spectra archive

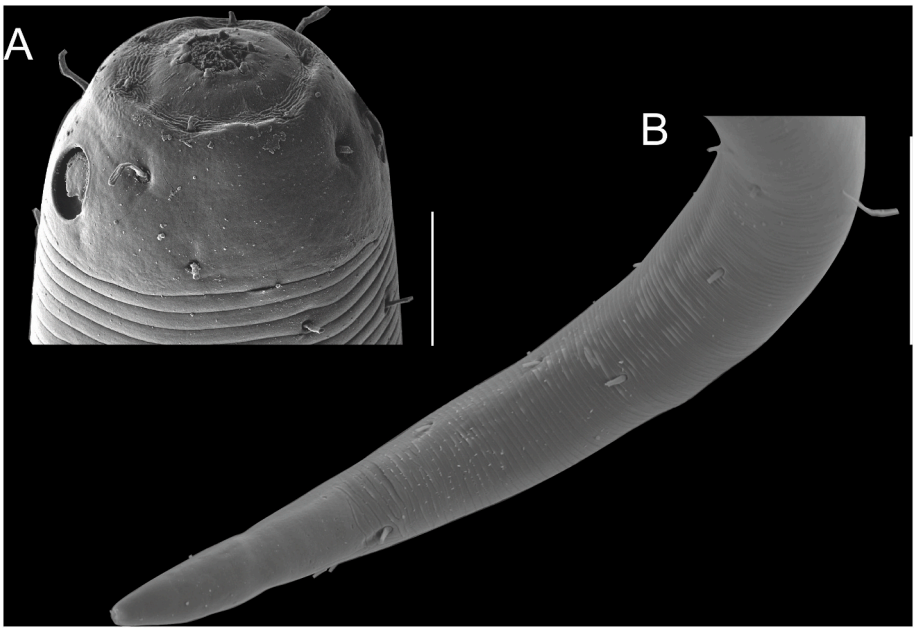

Fig. 6. *Desmodora hydrothermica* sp. nov. Female. SEM. A. Anterior end. B. Tail tip. Scale bars: A – 10 μm, B – 20 μm.

site (LipidWeb). Each fatty acid was quantified by calculating its peak area relative to the total peak area. These values are referred to as fatty acid content (%) throughout the paper. Absolute concentrations of FAs were not determined.

3. Results

3.1. Morphological analysis

Order Desmodorida De Coninck, 1965
Family Desmodoridae Filipjev, 1922
Genus *Desmodora* de Man (1889).

Generic diagnosis (from Leduc, 2021): Cuticle without ridges or spines. Cephalic capsule either smooth or partly to entirely ornamented with structures resembling pores or small vacuoles, which have been shown by scanning electron microscopy to not be visible on the cuticle surface; cephalic setae located either in the lip region or on main part of head capsule. Subcephalic setae sometimes present, when present few in number and mainly located posteriorly to amphideal fovea. Amphideal fovea cryptospiral or multispiral, seldom loop-shaped. Buccal cavity with large dorsal tooth and smaller subventral teeth. Pharynx with oval or circular posterior bulb. Spicules short, arcuate, with capitulum and velum. Precloacal supplements sometimes present, usually pore-like, seldom consisting of cuticular swellings or flaps. Tail usually conical, seldom conical-cylindrical.

Type species: *D. communis* (Butschli, 1874).

Remarks. A list of 35 valid species of the genus was provided by Leduc and Zhao (2016b)

***Desmodora hydrothermica* sp. n** (Figs. 3–6).

Type specimens. The male holotype, five male paratypes, and five female paratypes (No. MIMB44533); three male paratypes and ten female paratypes (No. MIMB44532).

Type Repository. All specimens were deposited in the Museum of the A.V. Zhirmunsky National Scientific Center of Marine Biology FEB RAS (Vladivostok, Russia).

Locality. Bering Sea, summits of the submarine Piip volcano (55.38° N, 167.26° E), depth 452–469 m, bottom sediments and hydrothermal carbonate chimneys.

Etymology. The species name is given by the type habitat of the nematode.

Measurements: See Table 2.

Description. Male. Long cylindrical body with slight reddish to brownish colour, rounded anterior end and slender conical tail. Cuticle coarsely annulated posterior to head capsule. Annuli without any spines. Striations at level of beginning of intestine more regular then in the tail. Lateral differentiation absent. Eight longitudinal rows of setae distributed symmetrically along entire body length and irregularly in caudal region. Setae in anterior region 2 μm long, at the posterior region they decrease to 1.5–1 μm. Body annuli slightly broader in pharyngeal region (about 3 μm) than along the rest of the body.

Cephalic capsule consists of two parts: thin, conical, non-vacuolated lip region (3–5 μm long) 'separated' with a suture from the thickly cuticularised, rectangular main part of the cephalic capsule (12–17 μm long) which is ornamented with numerous tiny vacuoles.

Six internal (difficult to observe) and six external labial papillae present on extendable portion of labial region, and four cephalic setae (5 μm long) located behind suture of cephalic capsule, anterior to amphid. Subcephalic setae absent. Some additional short somatic (cervical) setae can be present irregularly on the posterior part of cephalic capsule. Amphids (25–34% of corresponding diameter) situated laterally on main cephalic region; cryptospiral (1.1 turns) amphideal fovea located in middle of main region of cephalic capsule, amphideal fovea slightly wider than amphideal aperture.

Buccal cavity with a poorly developed dorsal tooth, ventrosublateral teeth not observed. Cylindrical muscular pharynx with slightly cuticularised lumen and oval posterior pharyngeal bulb. Secretory-excretory system not observed. Nerve ring slightly posterior to the middle of the pharynx. Cardia short, trapezium-shaped.

Reproductive system monorchic with anterior outstretched testis located ventrally to and at the left (testis tip) of the intestine. Large, globular sperm cells (23–18 × 25–27 μm) in size. Arched spicules with developed capitulum and broad velum. Laminar gubernaculum, without apophysis, composed of two equal short parts (17 μm long). No special cuticular appendages related to the male reproductive system.

Long, slender conical tail, non-annulated tail tip without perforations, 26–33 μm long. Caudal glands extending as far as the mid of the spicules.

Female. Similar to male, but with lower values of ratio *a*, and slightly smaller amphideal fovea. Reproductive system didelphic, amphidelphic with ventrally reflected ovaries located both to the left or to the right of

Table 2
Morphometrics (minimum-maximum/mean ± SD) of *D. hydrothermica* sp.*nov.*, *D. marci, D. spongiocola* sp.*nov.*, *D. spongiophila* sp.*nov*, Piip volcano. Measurements are in micrometers.

	Desmodora hydrothermica sp.nov.			Desmodora marci		Desmodora spongiocola sp.nov.			Desmodora spongiophila sp.nov.		
	Males		Females	Males	Females	Males		Females	Males		Females
	Holotype	Paratypes				Holotype	Paratypes		Holotype	Paratypes	
n		8	15	6	3		4	3		4	3
L	2089	1825–2189 2013 ± 103	1727–2358 1991 ± 174	2252–2629 2456 ± 127	2252–3013 2658 ± 383	2090	2050–2774 2457 ± 356	2094–2426 2292 ± 175	4007	3445–4442 3881 ± 407	3327–4194 3709 ± 443
A	28.6	30.9–45.6 36.5 ± 4.2	24.3–44.6 31.7 ± 6.4	25.8–40.2 30.4 ± 5.6	23.0–36.9 28.6 ± 7.4	39.4	39.4–55.4 46.5 ± 5.8	36.7–40.6 38.6 ± 2.0	66.8	60.7–90.7 69.84 ± 11.9	52.0–59.1 55.0 ± 3.7
B	10.1	9.2–10.5 9.7 ± 3.5	8.5–9.7 9.7 ± 0.5	10.1–11.5 10.6 ± 0.5	11.4–12.3 11.7 ± 0.5	8.6	8.1–10.0 9.3 ± 0.9	8.2–9.3 8.8 ± 0.6	14.7	12.8–15.3 13.8 ± 1.1	12.0–14.4 13.0 ± 1.2
C	9.0	9.4–10.8 10.1 ± 0.4	8.7–11.7 9.9 ± 1.0	8.1–9.8 8.9 ± 0.7	7.6–9.8 8.6 ± 1.1	10.0	10.0–12.5 11.1 ± 0.9	10.5–11.2 10.8 ± 0.4	25.5	23.2–29.8 26.4 ± 2.7	25.0–27.6 26.0 ± 1.4
c’	5.4	4.9–6.8 5.9 ± 0.6	5.6–8.0 6.8 ± 0.7	4.3–7.1 5.7 ± 1.0	6.7–7.6 7.2 ± 0.5	5.9	5.0–7.4 6.2 ± 0.9	6.5–8.0 7.4 ± 0.8		3.4–4.1 3.7 ± 0.4	4.3–4.8 4.5 ± 0.3
V, %			48.6–54.2 51.7 ± 1.7		47.1–48.4 47.9 ± 0.7			44.5–45.6 45.1 ± 0.6			47.4–49.9 48.5 ± 1.3
Head diam. at cephalic setae	32	26–33 28 ± 2	27–33 30 ± 2	36–49 46 ± 5	38–51 45 ± 6	33	32–34 33 ± 1	31–32 32 ± 1	31	31–32 32 ± 0.3	31–33 32 ± 1
Length of cephalic setae	5	4–5	4–6	8–12	7–9	7	6–7	6	8	8–10	6–9
Amphid width	8	7–8	7–11	8–11	8–10	10	10–11	10	8	7–8	7
Amphid width/ cbd (%)	25.8	25.7–34.9 30.2 ± 3.4	24.6–36.7 28.8 ± 3.4	25.4–38.7 29.6 ± 5.2	19.3–24.3 22.6 ± 2.9	34.6	34.6–35.4 34.9 ± 0.3	34.6–36.6 35.7 ± 1.0	26.8	26.8–30.4 28.2 ± 1.7	23.0–28.5 26.3 ± 2.9
Amphid from anterior end	8	7–10 9 ± 1	5–11 8 ± 2	9–13 10 ± 4	7–10 8 ± 1	10	7–10 8 ± 1	8–9 9 ± 1	8	7–9 8 ± 1	8–10 9 ± 1
Nerve ring from anterior end	133	102–143 127 ± 13	107–149 126 ± 10	123–146 138 ± 9	124–138 129 ± 7	140	140–188 161 ± 26	146–157 153 ± 6	175	150–177 167 ± 12	175–186 180 ± 6
Pharynx length	206	199–238 210 ± 14	186–224 204 ± 11	196–245 232 ± 18	197–244. 226 ± 25	242	242–279 264 ± 16	254–267 260 ± 7	272	270–297 281 ± 12	277–292 284 ± 8
Max. body diam.	73	48–61 56 ± 5	40–84 65 ± 14	56–102 83 ± 16	61–118 99 ± 33	53	45–59 53 ± 6	57–63 59 ± 3	60	49–61 56 ± 5	64–71 67 ± 4
Spicule length along arch	65	60–72 67 ± 5		63–87 74 ± 9		66	58–69 67 ± 6		50	45–50 48 ± 2	
Gubernaculum length		13–22 17 ± 5		18–29 25 ± 4		12	12–21 17 ± 4		17	17–18 17 ± 1	
Cloacal/anal body diam.	43	31–43 35 ± 4	24–36 30 ± 4	39–67 50 ± 10	39–46 43 ± 4	35	35–38 36 ± 1	25–33 29 ± 4	40	36–44 39 ± 3	28–33 31 ± 3
Tail length	233	187–211 200 ± 7	181–215 199 ± 10	245–304 276 ± 20	297–317 307 ± 10	208	191–260 222 ± 26	200–222 213 ± 11	157	139–157 147 ± 8	133–152 142 ± 10
Vulval body diam.			45–84 67 ± 11		61–118 99 ± 33			57–63 59 ± 3			53–67 62 ± 8

the intestine according to the specimen. Spermatheca not observed. Vulva is a broad transverse slit, located slightly posterior to mid-body. Proximal portion of vagina heavily cuticularised, surrounded by constrictor muscle. No vaginal glands observed.

Juveniles. Body shape, annuli, head capsule with ornamentation, position of cephalic setae, position and shape of fovea amphidealis, pharynx and intestine of all three stages found are similar to adults.

Diagnosis. *Desmodora hydrothermica* sp.nov. is characterized by rounded cephalic capsule with a wavy suture, eight longitudinal rows of somatic setae, cryptospiral amphideal fovea, buccal cavity with a poorly developed tooth, relatively long tail ($8.7 < c < 11.7$, $4.9 < c' < 8.0$), males without precloacal supplement, spicules with a cephalated proximal end.

Differential diagnosis. *Desmodora hydrothermica* sp. nov. resembles *D. alberti* Verschelde et al., 1998, *D. granulata* Vincx and Gourbault (1989) and *Desmodora spongiocola* sp. nov. *D. hydroterma* sp.nov. can be easily distinguished from *D. alberti* and *D. granulata* by its body size (1.7–2.5 mm *vs* 0.8–1.2 mm and 1.04–1.3 mm, respectively). Moreover, *Desmodora hydrothermica* sp.nov. can be distinguished from *D. alberti* by the number of longitudinal rows of somatic setae (8 *vs* 6). *Desmodora hydrothermica* sp.nov. can be distinguished from *D. granulata* by the length of spicules (60–72 μm *vs* 44–46 μm). *Desmodora spongiocola* sp. nov. differs from *Desmodora hydrothermica* sp.nov. by the well-developed buccal cavity with a hollow forwardly directed dorsal tooth and 2 min ventrosublateral teeth, by the position of amphideal fovea at the anterior area of cephalic capsule, in the length of non-annulated tail tip (17–23 *vs* 26–33).

Nucleotide sequences. GenBank accession numbers OM108626-OM108629 (18S rDNA), OM274098-OM274101 (28S rDNA).

Desmodora marci Verschelde et al., 1998 (Figs. 7–10).

Material examined. Eight males and three females.

Locality: Bering Sea, submarine Piip volcano, (55.38° N, 167.26° E), depth about 469 m. Washout from bottom sediments with mussels *Calyptogena pacifica*.

Measurements: see Table 2.

Description. Male. Long cylindrical and robust body with brownish colour, rounded anterior end and long, slender tail. Cuticle coarsely annulated posterior to head capsule. Distinctly annulated cuticle with annules (without any spines) more widely spaced in pharyngeal region than on rest of body. Striations become irregular toward the tail with non-annulated tip. Lateral differentiation absent. Short somatic setae (3–5 μm length) arranged in eight longitudinal rows along entire body length. The surface of the body is often covered with bacteria of various shapes (Fig. 10C, D, G).

Anterior sensilla presented by six internal and six external labial papillae, and four cephalic setae (8–12 μm) at level of the anterior edge of the fovea amphidealis. There is an additional irregular circle of about eight somatic (cervical) setae at the base of the cephalic capsule or just

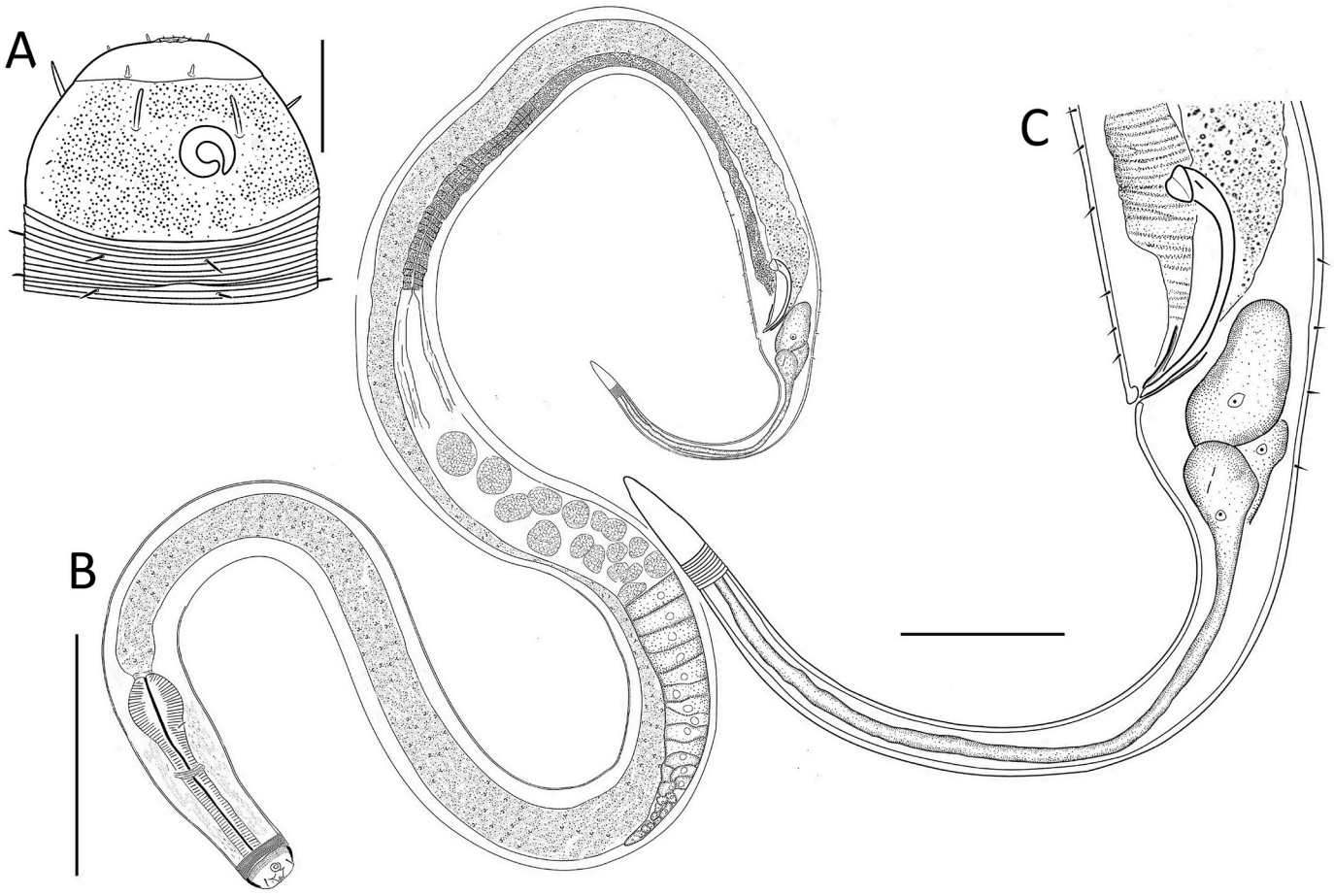

Fig. 7. *Desmodora marci*. Male. A. Cephalic region. B. General view. C. Tail. Scale bars: A – 20 μm, B – 200 μm, C – 50 μm.

posterior to it. A short anterior retractable lip region separated from a larger posterior main cephalic region by a suture of an extra layer of thick cuticle. Main cephalic capsula usually wider than lip region and ornamented with numerous tiny vacuoles. Cryptospiral (1.1 turns) amphideal fovea located in middle of main region of cephalic capsule, amphideal fovea slightly wider than amphideal aperture. Amphids reach 39% of corresponding diameter.

Buccal cavity with visible dorsal tooth, ventrosublateral teeth not observed. Nerve ring at the level of two-thirds of pharynx. Cardia short. Muscular pharynx with large oval bipartite terminal bulb and cuticularised lumen.

Monorchic reproductive system located ventrally to and at the left (testis tip) of the intestine. Long arched spicules (63–87 μm) with developed capitulum and broad velum. Laminar short simple gubernaculum, without apophysis. No special cuticular appendages related to the male reproductive system. Long, slender conical-cylindrical tail, non-annulated tail tip without perforations, (about 10 μm) long. Three caudal glands and spinneret present, with opening divided internally by membrane.

Female. Similar to male, but with lower values of ratio *a*, and slightly smaller amphideal fovea and cephalic capsule. Reproductive system didelphic, amphidelphic with reflexed ovaries both located to right of intestine. Spermatheca not observed. Vulva located slightly posterior to mid-body. Proximal portion of vagina heavily cuticularised and colored. No vaginal glands observed.

Remarks. The specimens from the submarine Piip volcano are broadly similar to the original description of Verschelde et al. (1998) from the East Pacific Rise and the description of Tchesunov (2015) from Lucky Strike on the Mid-Atlantic Ridge. There is a difference in the number of rows of somatic setae, which are poorly distinguishable in most specimens. All the measurements and ratios coincide or largely overlap (Appendix Table 1).

Nucleotide sequences. GenBank accession numbers OM108623-OM108624 (18S rDNA), OM274095-OM274096 (28S rDNA).

Desmodora spongiophila* sp.*nov (Figs. 11–13).

Type specimens. The male holotype, four male paratypes, and three female paratypes (No. MIMB44534).

Type Repository. All specimens were deposited in the Museum of the A.V. Zhirmunsky National Scientific Center of Marine Biology FEB RAS (Vladivostok, Russia).

Locality. Bering Sea, the submarine Piip volcano (55.38° N, 167.26° E), depth 395–783 m, Hexactinellida and Demospongiae, bottom sediments, hydrothermal carbonate chimneys.

Etymology. The species name is given by the type habitat of the nematode, individuals of the new species were often found on the sponges.

Measurements: see Table 2.

Description. Male. Long cylindrical body with reddish to brownish colour, rounded anterior end and tapered tail. Coarsely annulated cuticle with annules more widely spaced in pharyngeal region than on rest of body. Annuli without any spines. Somatic setae (3–5 μm long) arranged in eight longitudinal rows along entire body length. A labial retractable region is separated from an extra thick and high cephalic capsule ornamented with tiny vacuoles.

Six inner and six outer labial papillae present on extendable portion of labial region, outer labial papillae 2 μm long. Four cephalic setae (8.3–10.2 μm long) present at the level of the anterior edge of the amphideal fovea. Eight long sub-cephalic setae (7–10 μm long, two

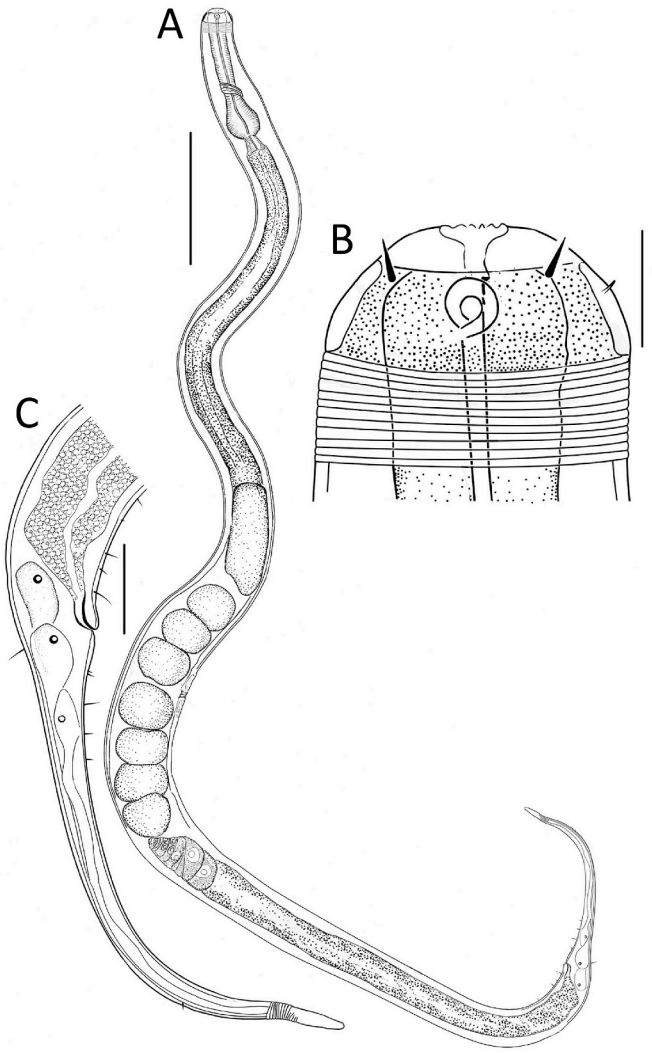

Fig. 8. *Desmodora marci*. Female. A. General view. B. Cephalic region. C. Tail. Scale bars: A – 200 μm, B – 20 μm, C – 50 μm.

subventral, two subdorsal, two ventro-sublateral and two dorsosublateral) located at level of the posterior edge of the amphideal fovea. Cryptospiral amphideal fovea (1.1 turns) located in the anterior area of cephalic capsule, amphideal fovea wider than amphideal aperture. Amphids 27% of corresponding body diameter. Buccal cavity with large cuticularised dorsal tooth and two small ventrosublateral teeth. Cylindrical pharynx with cuticularised lumen, posteriorly enlarged. Nerve ring encircles pharynx immediately to anterior this enlargment. Secretory-excretory system not observed. Reproductive system monorchic with outstretched testis located to left or right of intestine. Short, strongly curved spicules with well-developed capitulum and ventral alae. The gubernaculum is small and plate-like. Nine-eleven midventral supplements present. Posteriormost supplement consists of a rounded cuticular extension and located about 20 μm anterior to cloacal aperture, preceded by eight-ten small, pore-like supplements. Distance between supplements about 15–25 μm. Non-annulated tail tip about 15 μm long. Three caudal glands present, their nuclei are incaudal; spinneret with double opening at posterior extremity of tail.

Female. Similar to male, but with lower values of ratio a, and slightly smaller amphideal fovea. Reproductive system didelphic, amphidelphic with reflexed ovaries both located to right of intestine. Spermatheca not observed. Vulva located slightly anterior to mid-body. Proximal portion of vagina heavily cuticularised and surrounded by constrictor muscle. No vaginal glands observed.

Diagnosis. *Desmodora spongiophila* sp. nov. is characterised by a long body, eight longitudinal rows of somatic setae of medium length (3–5 μm), eight sub-cephalic setae on cephalic capsule, cryptospiral amphideal fovea (1.1 turns), males with nine-eleven precloacal midventral supplements (one mound-shaped and eight-ten pore-like).

Differential diagnosis. *Desmodora spongiophila* sp. nov. can be differentiated from all other species of the genus by its body length (3327–4442 μm). This new species resembles *D. bilacinia* Leduc and Zhao, 2016b, *D. communis* (Bütschli, 1874), *D. deconincki* (Inglis, 1968) and *D. septentrionalis* Kreis (1963) in the presence of sub-cephalic setae and somewhat similar precloacal supplements.

Desmodora spongiophila sp. nov. can be distinguished from *D. bilacinia* by the structure (mound-shaped and pore-like *vs* rounded cuticular extensions) and number (9–11 *vs* 2) of precloacal supplements, by the absence of two rows of thick subventral setae extend from precloacal supplements to near tail tip.

Desmodora spongiophila sp. nov. differs from *D. communis* and *D. septentrionalis* by the number of sub-cephalic setae (8 *vs* 4), in the structure and number of precloacal supplements (9–11 *vs* 12–13 and 9–11 *vs* 6 respectively).

Desmodora spongiophila sp. nov. differs from *D. deconincki* by the number of precloacal supplements (9–11 *vs* 1).

Nucleotide sequences. GenBank accession numbers OM108625 (18S rDNA), OM274097 (28S rDNA).

***Desmodora spongiocola* sp.nov.** (Figs. 14–16).

Type specimens. The male holotype, four male paratypes, and three female paratypes (No. MIMB44535).

Type Repository. All specimens were deposited in the Museum of the A.V. Zhirmunsky National Scientific Center of Marine Biology FEB RAS (Vladivostok, Russia).

Locality. Bering Sea, the submarine Piip volcano (55.38° N, 167.26° E), depth 395–783 m, Demospongiae, bottom sediments.

Measurements: see Table 2.

Etymology. The species name is given by the type habitat of the nematode, individuals of the new species were often found on the sponges.

Description. Male. Long cylindrical and robust body with brownish colour, rounded anterior end and cylindrico-conical tail. Cuticle coarsely annulated posterior to cephalic capsule. Distinctly annulated cuticle with annules (without any spines) more widely spaced in pharyngeal region than on rest of body. Striations become irregular toward the tail with non-annulated tip. Lateral differentiation absent. Fine somatic setae (3–5 μm long) arranged symmetrically in eight longitudinal rows along entire body length.

Six internal papilliform labial sensilla, six external setiform sensilla (3 μm), and four cephalic setae (6 μm) located on the cephalic capsule at the anterior border of amphideal fovea. Main cephalic region usually wider than lip region and ornamented with numerous tiny vacuoles. Cryptospiral amphideal fovea (1.2 turns) located in the anterior area of the cephalic capsule, amphideal fovea slightly wider than amphideal aperture. Amphids about 35% of the corresponding diameter of the capsule. 1–2 circles of the somatic setae on the posterior area of the cephalic capsule. Cylindrical pharynx with elongate posterior bulb and weakly cuticularised lumen. Well-developed buccal cavity with a hollow, forwardly directed, dorsal tooth and 2 min ventrosublateral teeth at the same level. The distance from the anterior edge of the body to the nerve ring is 130 μm. Cardia short.

Monorchic reproductive system located ventrally to and at the left (testis tip) of the intestine. Mature large globular sperm cells, 3 × 4 μm in size. Slender and ventrally curved spicules, with small rounded capitulum. The gubernaculum is plate-shaped, without apophysis. No special cuticular appendages related to the male reproductive system. Three caudal glands present, their nuclei are incaudal; spinneret with single opening. Tail conical, non-annulated tail tip long size (15–20 μm) without perforations.

Female. Similar to male, but with lower values of ratio *a*.

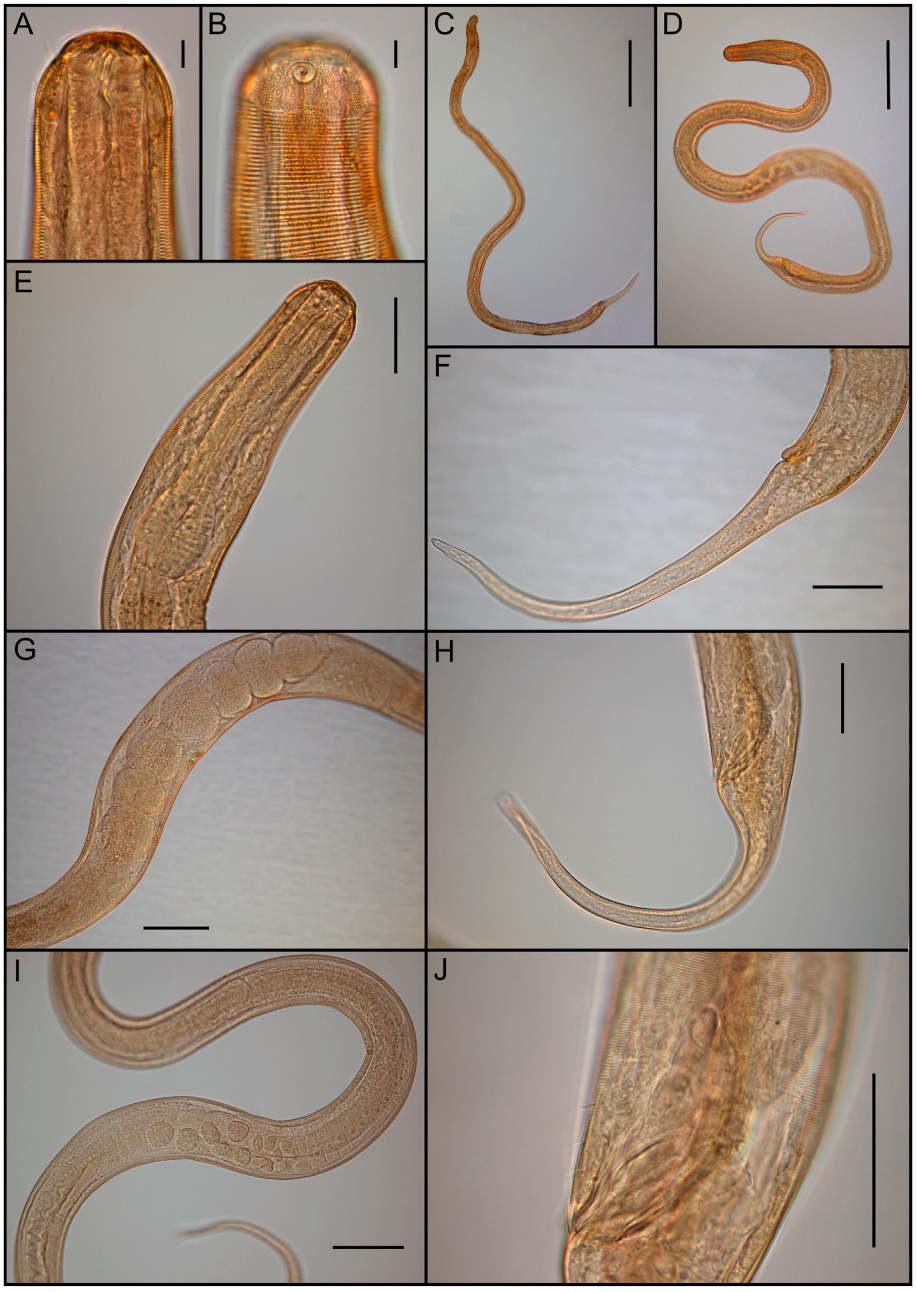

Fig. 9. *Desmodora marci.* Light microscopy, DIC. A. Cephalic region of female. B. Cephalic region of male. C. Juvenile body. D. Male body. E. Female anterior region. F – female tail. G. Female reproductive system. H. Male tail. I. Testis. J. Male copulatory apparatus. Scale bars: A, B – 10 μm; C – 200 μm; D – 300 μm; E, F, H, J – 50 μm; G, I – 100 μm.

Reproductive system didelphic, amphidelphic with reflexed ovaries both located to right of intestine. Spermatheca not observed. Vulva located slightly anterior to mid-body.

Diagnosis. *Desmodora spongiocola* sp.nov. is characterized by its long cephalic capsule; by eight longitudinal rows of somatic setae of medium length; by cryptospiral amphideal fovea at the anterior area of cephalic capsule; by well-developed buccal cavity with a hollow forwardly directed dorsal tooth and 2 min ventrosublateral teeth; by cylindrical pharynx with elongate posterior bulb and weakly cuticularised lumen; by conical tail and spinneret with single opening; by absence of alae and copulatory supplements.

Differential diagnosis. *Desmodora spongiocola* sp.nov. resembles *D. alberti*, *D. granulate* and *Desmodora hydrothermica* sp. nov in the general shape of the body and in the absence of alae and copulatory supplements. However, the combination of some features of the new species is markedly different, including a long cephalic capsule and position of amphideal fovea at the anterior area of cephalic capsule. *Desmodora spongiocola* sp.nov. can be easily distinguished from *D. alberti* and *D. granulata* by its body size (2.1–2.8 mm *vs* 0.8–1.2 mm and 1.04–1.3 mm, respectively). *Desmodora spongiocola* sp.nov. differs from *D. alberti* by the number of longitudinal rows of somatic setae (8 *vs* 6). *Desmodora spongiocola* sp.nov. can be distinguished from *D. granulata* by the length of spicules (58–69 μm *vs* 44–46 μm).

Nucleotide sequences. GenBank accession numbers OM108630-OM108634 (18S rDNA), OM274102- OM274106 (28S rDNA).

3.2. Molecular analysis

A total of 12 samples were sequenced for 18S and D2-D3 region of 28S rDNA (voucher numbers BS31-BS33, BS51-BS54, BS59-BS63). The

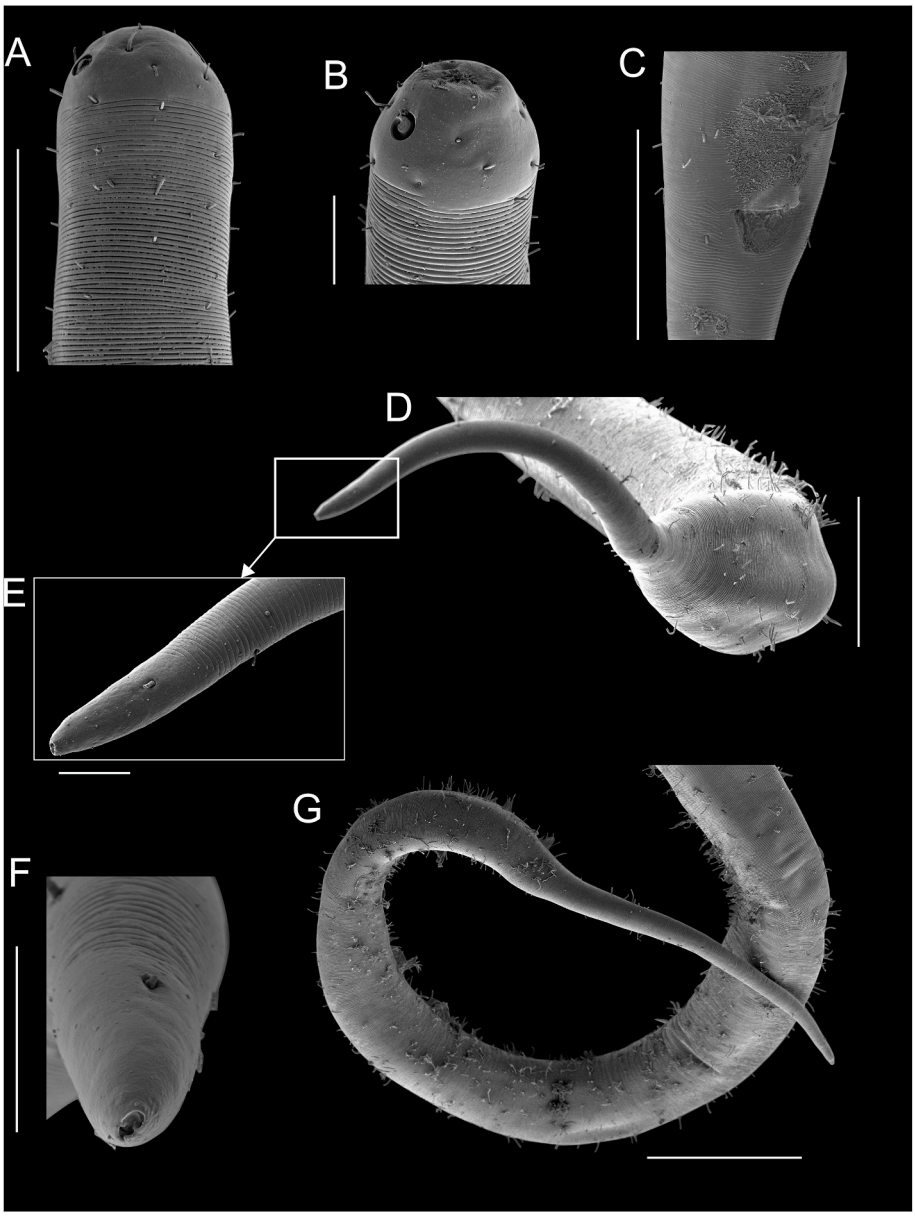

Fig. 10. *Desmodora marci*. Female. SEM. A. Anterior region. B. Cephalic region. C. Anus. D. Tail. E, F. Tail tip. G. Posterior region. Scale bars: A, C, D – 50 μm; B – 20 μm; E, F – 10 μm; G – 100 μm.

final alignment of the 18S rDNA yielded 1504–1618 bp and 683–698 bp for 18S and 28S respectively. According to the morphological analysis (see above), the obtained samples belong to 4 species: BS31–BS32 – *Desmodora marci*, BS33 – *Desmodora spongiophila* sp.nov., BS51–BS54 – *Desmodora hydrothermica* sp.nov. and BS59–BS63 – *Desmodora spongiocola* sp.nov. The total pairwise p-distances within each species were in the range 0.0–0.4% and 0.0–0.5% for 18S and 28S respectively which shows that all sequences belong to the corresponding species. The results of interspecific distances of all obtained sequences are summarized in Table 3. The high distances between the studied species confirm their validity (Pereira et al., 2010; Armenteros et al., 2014a).

Among the members of the family Desmodoridae the primary clade was well supported (Bayesian posterior probability, PP = 1; Maximum likelihood bootstrap value percent, ML = 100) and formed by unidentified species of the genera *Catanema* and *Robbea* (Fig. 17). Bayesian inference (BI) phylogeny revealed a moderately polytomy node (PP = 0.54, ML = 11), including 3 primary clades of Desmodoridae: *Laxus* (PP = 1), *Leptonemella* + Stilbonematinae gen sp. (PP = 0.8, ML = 32) and the remaining members of the family. The earliest branching lineages of the remaining nematodes was *Stilbonema* (PP = 1, ML = 94), 3 species of genus *Robbea* (PP = 1, ML = 58) and *Eubostrichus* (PP = 1, ML = 81). The next clade (PP = 1, ML = 97) includes obtained sequence of *Desmodora spongiophila* sp.nov BS33. Four species, *Desmodora communis*, *Acanthopharynx* sp., *Acanthopharynx micans* and *Zalonema* sp. were placed as a sister to the sample BS33. After a clade consisted of *Metachromadoroides* and *Metachromadora* (PP = 0.84, ML = 90), Bayesian inference phylogeny revealed two sister clades (PP = 0.98). The first clade (PP = 0.56) includes members of the genera *Desmodora*, *Desmodorella* and *Chromaspirina*. The new species *Desmodora spongiocola* sp. nov. (PP = 1, ML = 100) was places as sister to *Spirinia*. The second clade (PP = 0.62) includes the remaining *Desmodora* species as well as *Pseudochromadora*, *Desmodorella* and *Metachromadora*. Obtained sequences of *Desmodora marci* were conspecific to *Desmodora marci* and *Desmodora hydrothermica* was conspecific to *Desmodora* sp. JX463181.

In the D2-D3 of LSU phylogenetic tree the primary clade was formed by the genera *Pseudochromadora* (Fig. 18), whereas the position of

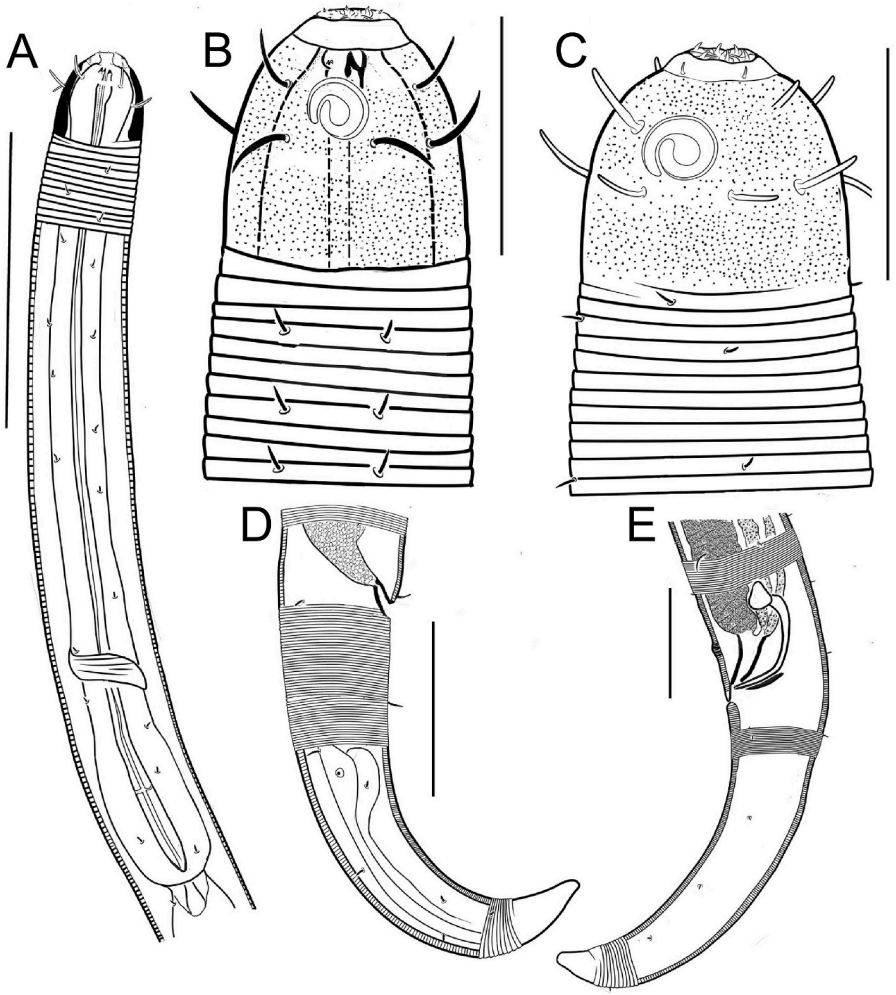

Fig. 11. *Desmodora spongiophila* sp.nov. A. Anterior region of female. B. Female cephalic region. C. Male cephalic region. D. Female tail. E. Male tail. Scale bars: A – 100 μm; B, C – 30 μm; D, E – 50 μm.

sequences of new species and support of the clades generally corresponded to the topology revealed Bayesian Inference on 18S rDNA.

3.3. Stable isotopes and fatty acids analysis

The $\delta^{13}C$ and $\delta^{15}N$ values of nematodes, sediment organic matter (SOM) and microbial mats are presented in Table 4 and Fig. 19. SOM $\delta^{13}C$ values ranged from −26.4‰ to −23.4‰, and $\delta^{15}N$ values ranged from 1.9 to 4.4‰ for areas with and without of *Calyptogena pacifica* respectively. The $\delta^{13}C$ and $\delta^{15}N$ mean values of microbial mats were −31.5‰ and 6.4‰, respectively.

The nematode $\delta^{13}C$ values ranged from −44.5 (*Desmodora spongiophila* sp.nov., station 7) to −19.4‰ (*Desmodora spongiophila* sp.nov., station 2), and the $\delta^{15}N$ values ranged from 2.5 (*D. marci*, station 6) to 12.7‰ (Nematoda, station 2).

The $\delta^{13}C$ and $\delta^{15}N$ values of *Desmodora* samples from hydrothermal habitats were lower than the values of nematode samples from habitats outside of hydrothermal activity. The *Desmodora hydrothermica* sp.nov. from hydrothermal chimneys were characterized by significantly depleted $\delta^{13}C$ and $\delta^{15}N$ relative to nematodes from station 7 (Tukey's pairwise tests, $p < 0.001$).

Among-site differences were observed for *Desmodora hydrothermica* sp.nov and *Desmodora spongiophila* sp.nov. There were no significant among-site differences in *D. hydrothermica* sp.nov. $\delta^{13}C$ values, but $\delta^{15}N$ values were different (Tukey's pairwise tests, $p = 0.009$). *Desmodora spongiophila* sp.nov. $\delta^{13}C$ and $\delta^{15}N$ values were characterized by very high variation and ranged from −44.5 to −19.4‰, and from 7.7 to 10.7‰, respectively. In general, the values of isotopic signatures increased with distance from hydrothermal vents.

The fatty acid composition of *Desmodora hydrotherma* sp.nov. demonstrated the strong dominance of monounsaturated fatty acids (MUFAs) (60–66%), 16:1n-7 and 18:1n-7 together account for 47–53% of FAs (Table 5). Saturated fatty acids (SFAs) varied from 23% to 29%, and polyunsaturated fatty acids (PUFAs) were found in very low abundance (7–9%).

4. Discussion

4.1. Morphological and molecular analysis

The identification of nematodes of the genus *Desmodora* is challenging as these animals demonstrate a limited number of useful differential morphological characters. Moreover, *Desmodora* species, like other Desmodorinae genera, often occur together. (Verschelde et al., 1998; Moura et al., 2014; Zograf et al., 2021). The inability to unambiguously distinguish species makes it difficult to conduct research at the species level, study nematode communities, inventory biological diversity, analyze spatial distribution, identify biogeographic patterns, etc.

Some features, important for species identification, are practically invisible under a light microscope and require a scanning electron microscope such as: structure of the spinnneret, number and structure of

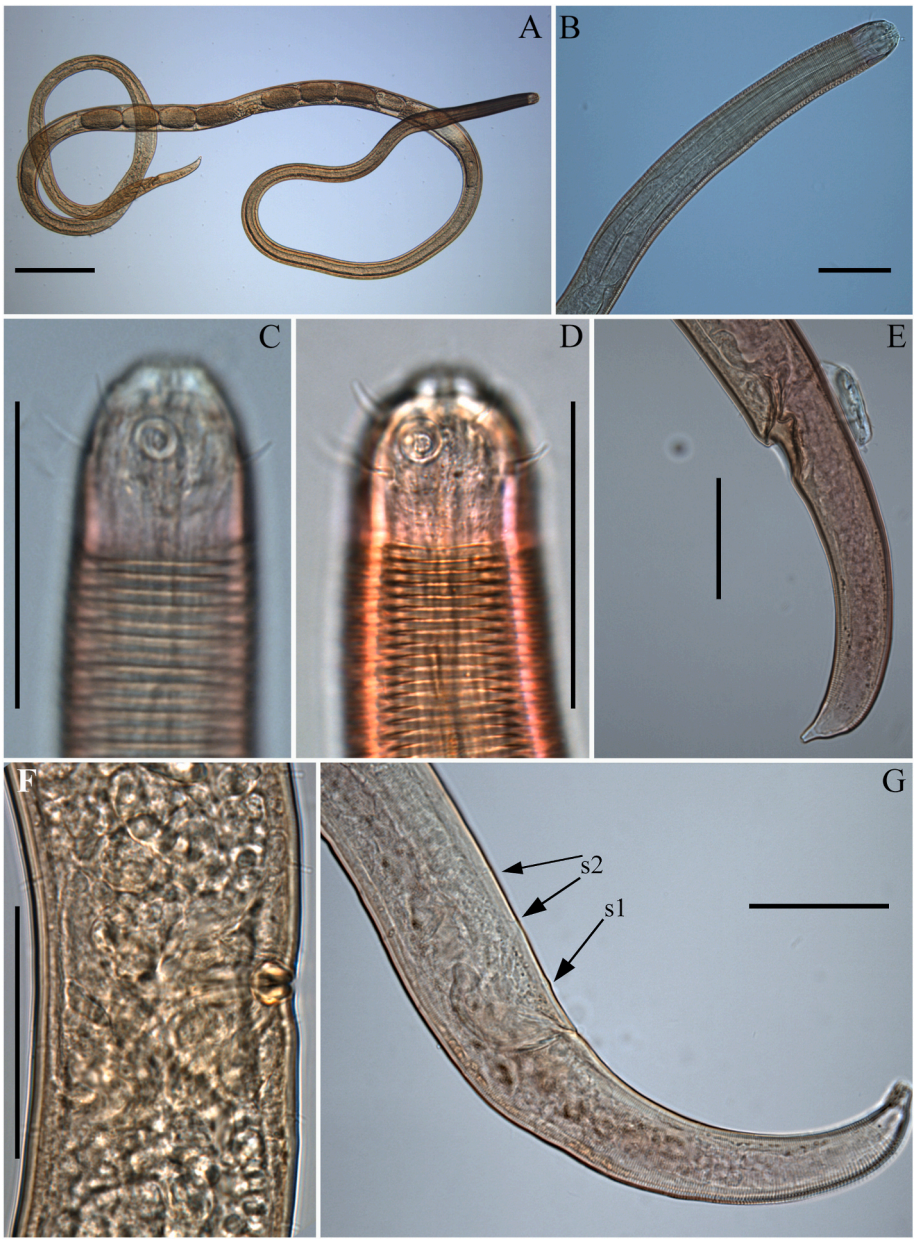

Fig. 12. *Desmodora spongiophila* sp.nov. Light microscopy, DIC. A. Female body. B. Female anterior region. C. Female cephalic region. D. Male cephalic region. E. Female tail. F. Vulva region. G. Female posterior region (s1 – mound-shaped precloacal supplement, s2 – pore-like precloacal supplements). Scale bars: A – 200 μm; B-G – 50 μm.

male supplements, number and location of sensilla. This was also shown for the species studied in the work. The use of an integrative approach based on genetic and detailed morphological studies makes it possible to overcome difficulties in species identification (Derycke et al., 2005, 2010; De Oliveira et al., 2012). The results of morphological studies, as well as DNA barcoding confirm the validity of the species we have described. Unfortunately, for many species described in the past, there are no detailed morphological descriptions, as well as nucleotide sequences. Publications of this kind, with modern redescriptions, seem to be quite relevant and in demand.

The genus *Desmodora* was established by de Man (1889) based on the species *Spilophora communis* Bütschli, 1874 from the Kiel Bay. Several taxonomic studies dealt with taxa of the Desmodorinae and revisions (and/or identification keys) for *Desmodora* have been published (Gerlach, 1950, 1963; Wieser, 1954; Boucher, 1975; Verschelde et al., 1998, 2006; Armenteros et al., 2014b; Moura et al., 2014; Leduc and Zhao, 2016a). Verschelde et al. (1998) proposed a taxonomic revision of *Desmodora* together with an emended generic diagnosis and reinstated subgenera as genera and reviewed the taxonomic composition of the genus by changing the status of some species. This revision was well confirmed by morphological data. However, the molecular phylogenetic analysis did not support the monophyly of *Desmodora* (Armenteros et al., 2014a; Leduc and Zhao, 2016a, b). Our SSU and D2-D3 of LSU phylogenetic trees largely agree with those of previous analyses indicating that *Desmodora* is not monophyletic. Moreover, phylogenetic relationships within the subfamily Desmodorinae remain unresolved.

Misidentification may be one of the reasons for the unrealistic genetic distances observed in some species and genera of Desmodorinae (Armenteros et al., 2014a; Zograf et al., 2021). At the same time, it is obvious that the observed topology of phylogenetic trees contradicts the taxonomy of the subfamily based on morphological data. The presented results are preliminary; to resolve the contradictions, it is necessary to

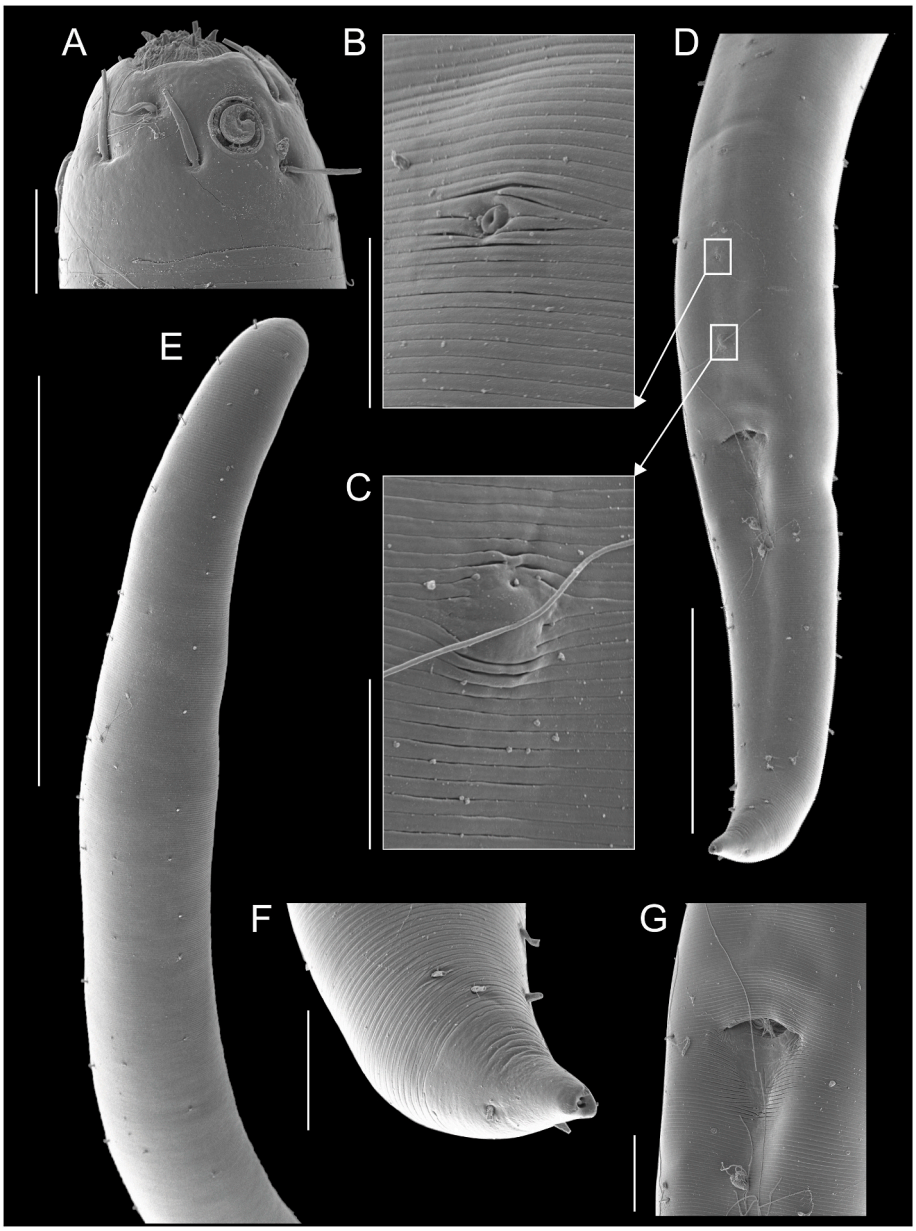

Fig. 13. *Desmodora spongiophila* sp.nov. Male. SEM. A. Cephalic region. B. Second copulatory supplement. C. Posteriormost copulatory supplement. D. Posterior region, ventral view. E. Posterior region, dorsal view. F. Tail tip. G. Cloaca region. Scale bars: A, F, G – 10 μm; B, C – 5 μm; D –50 μm; E – 100 μm.

include a larger number of species, genera, and molecular markers in the analysis. A more recent detailed analysis of morphological features and their significance is also required.

4.2. Spatial distribution

Individuals of *Desmodora* have been found in most of the studied habitats on the summits of the Piip volcano. The species often lived together, but a pronounced spatial specialization was observed. *Desmodora spongiophila* sp.nov. and *Desmodora spongiocola* sp.nov. were abundant inhabitants of the vulcanellids and some hexactenellids common on the volcano. *Desmodora hydrothermica* sp.nov. dominated in microbial mats on the carbonate chimneys from the South Summit, while *Desmodora marci* was found on stones near vents and in bottom sediments with vesicomyid *Calyptogena pacifica*.

Desmodora marci and *Desmodora hydrothermica* sp.nov. were already known in deep-sea reduced environments of the Pacific and Atlantic oceans, in similar habitats. Specimens of *Desmodora marci* were previously sampled from the collection box containing two species of bivalves, *Bathymodiolus* mussels and a species of *Acharax*, taken from hydrothermal vents in the Lau Basin in the South-West Pacific (Verschelde et al., 1998), from a piece of a sulphide tube overgrown with mussels *Bathymodiolus azoricus* in hydrothermal sites of North Mid-Atlantic Ridge (Tchesunov, 2015) and from carbonate rocks and sulphide-oxidizing bacterial mats at Hydrate Ridge methane seeps (off the coast of Oregon, North-East Pacific) (Sapir et al., 2014). Nucleotide sequence identical *Desmodora hydrothermica* sp.nov. (Fig. 17), was obtained from the same carbonate rocks and sulphide-oxidizing bacterial mats at Hydrate Ridge methane seeps and were identified as *Desmodora* sp. 9 (Sapir et al., 2014). These results may indicate the presence of a specialized nematofauna of deep-sea reducing habitats at the species level. In addition, the results confirm the suggestion that some species of deep-sea nematodes can be characterized by an extremely wide spatial distribution (Mordukhovich et al., 2019).

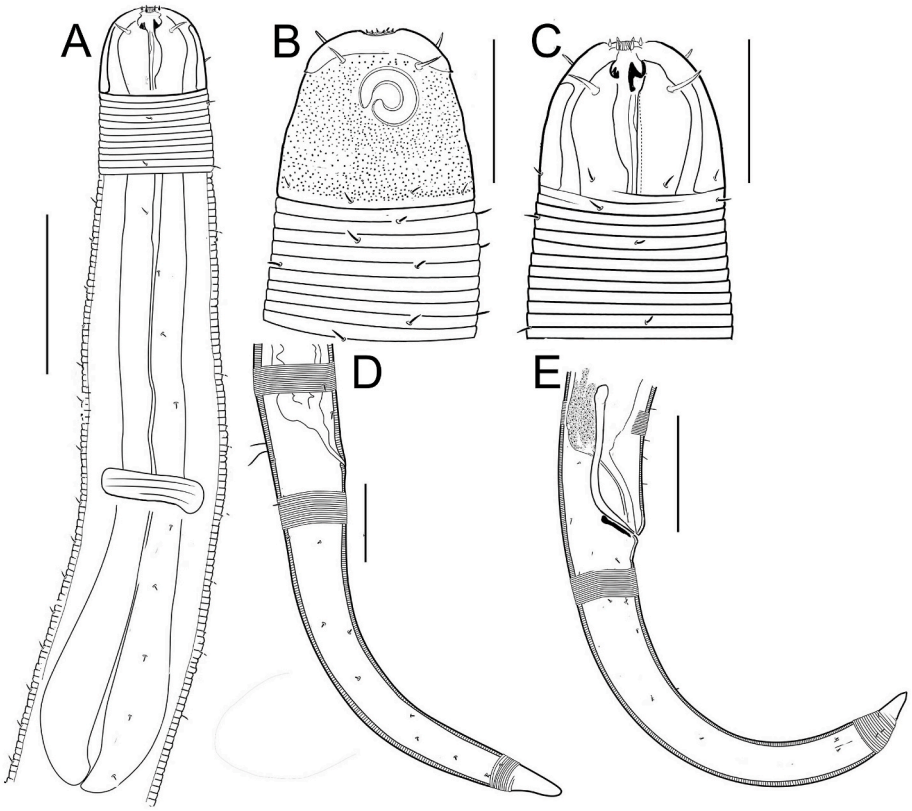

Fig. 14. *Desmodora spongiocola* sp.nov. A. Female anterior region. B. Female cephalic region. C. Male cephalic region. D. Female tail. E. Male tail. Scale bars: A, D, E – 50 μm; B, C – 30 μm.

4.3. Trophoecological studies

The $\delta^{13}C$ and $\delta^{15}N$ values of SOM (Fig. 19, Table 4) showed high variation between stations and reached ranges from −26.4 to −23.3‰ for $\delta^{13}C$ and from 1.9 to 4.4‰ for $\delta^{15}N$. Such variability may be the result of the variation in the contribution of organic matter of chemosynthetic origin (higher for the area with *Calyptogena pacifica*). The $\delta^{13}C$ and $\delta^{15}N$ mean values of SOM at similar depths in the Bering Sea outside reducing environment were −22.3‰ and 5.9‰, respectively (Kiyashko & Mordukhovich, unpubl.). In this way, SOM at station 7 was characterized by slightly depleted $\delta^{13}C$ and $\delta^{15}N$. It seems that organic matter of photosynthetic origin prevails at this station, but there is also a pronounced influx of chemosynthetic organic matter. Interpretation of the obtained results should be approached with caution, as the isotopic signatures at station 7 were determined from the a single sample.

Nematodes at station 7 were isotopically heavier relative to bulk SOM (−20.8‰ *vs* −23.9‰ for $\delta^{13}C$ and 12.5‰ *vs* 4.4‰ for $\delta^{15}N$). Stable nitrogen isotope ratios of consumers are typically enriched by 3.4‰ relative to their diet (Wada et al., 1993; Post, 2002; Fry, 2006). Thus, the heavy isotope enrichment of nematode samples is likely to be a result of feeding on organic matter that has been transformed by microheterotrophs and is associated with an increase in the number of trophic levels.

The most abundant species from carbonate hydrothermal chimneys, the nematode *D. hydrothermica* sp.nov., was characterised by a FAs profile indicative of a bacterial diet (Table 5): strong dominance of MUFAs (16:1n-7 and 18:1n-7 together account for 47–53% of FAs) and very low abundance of n-3 and n-6 long-chain polyunsaturated FAs (commonly originating from photosynthetic plankton). The FA composition of *D. hydrothermica* sp.nov. from Piip voulcano is very similar to *Halomonhystera disjuncta* collected at the Håkon Mosby Mud Volcano (Van Gaever et al., 2009). It is known that 16:1n-7 and 18:1n-7 can be derived from diatoms (e.g. Dijkman and Kromkamp, 2006; Volkman, 2006), however, in deep-sea habitats, high levels of ω7 monounsaturated fatty acids have been found in invertebrates with bacterial symbionts (Kelly and Scheibling, 2012 and references therein) and in meiobenthic invertebrates that feed on chemosynthetic bacteria (Van Gaever et al., 2009).

The $\delta^{13}C$ and $\delta^{15}N$ values of *Desmodora* samples from hydrothermal habitats were greatly lower than the values of nematode samples from habitats outside of the hydrothermal activity. *Desmodora hydrothermica* sp.nov. from hydrothermal chimneys were characterized by significantly depleted $\delta^{13}C$ and $\delta^{15}N$ relative to nematodes from station 7 (Tukey's pairwise tests, $p < 0.001$). The depleted isotopic signatures confirmed the consumption of chemosynthetically derived organic matter (Levin and Michener 2002; Levin, 2005). Other studied samples of *Desmodora*, apart from *Desmodora spongiophila* sp.nov. at station 1, also demonstrate $\delta^{13}C$ values consistent with contributions to nutrition from chemosynthesis. At the same time, the values of isotopic signatures do not confirm that studied *Desmodora* species feed on sulfur-oxidizing bacteria that form microbial mats common on hydrothermal chimneys and hard substrata of the volcano. Samples of *Desmodora* had $\delta^{13}C$ and $\delta^{15}N$ close to or even more depleted than studied microbial mats. Reducing habitats are characterized by the presence of diverse microbial communities and the isotopic signatures of different microbial taxa can vary significantly (Levin and Michener 2002; Teske, 2010; Dick et al., 2013; Speth et al., 2022). It seems that the studied nematodes may have a high trophic selectivity.

All studied species have a stoma and well-developed digestive system, light microscopy did not reveal any structures that could be associated with endosymbionts. Scanning electron microscopy revealed the usual presence of ectosymbionts on *Desmodora marci* (Fig. 10D, G) and *Desmodora spongiocola* sp.nov. (Fig. 16J). However, ectosymbionts were not found in all individuals, and the degree of their development also varied greatly. The feeding strategy of these species, like the other two, remains unclear. The $\delta^{13}C$ values of *Desmodora spongiophila* sp.nov.

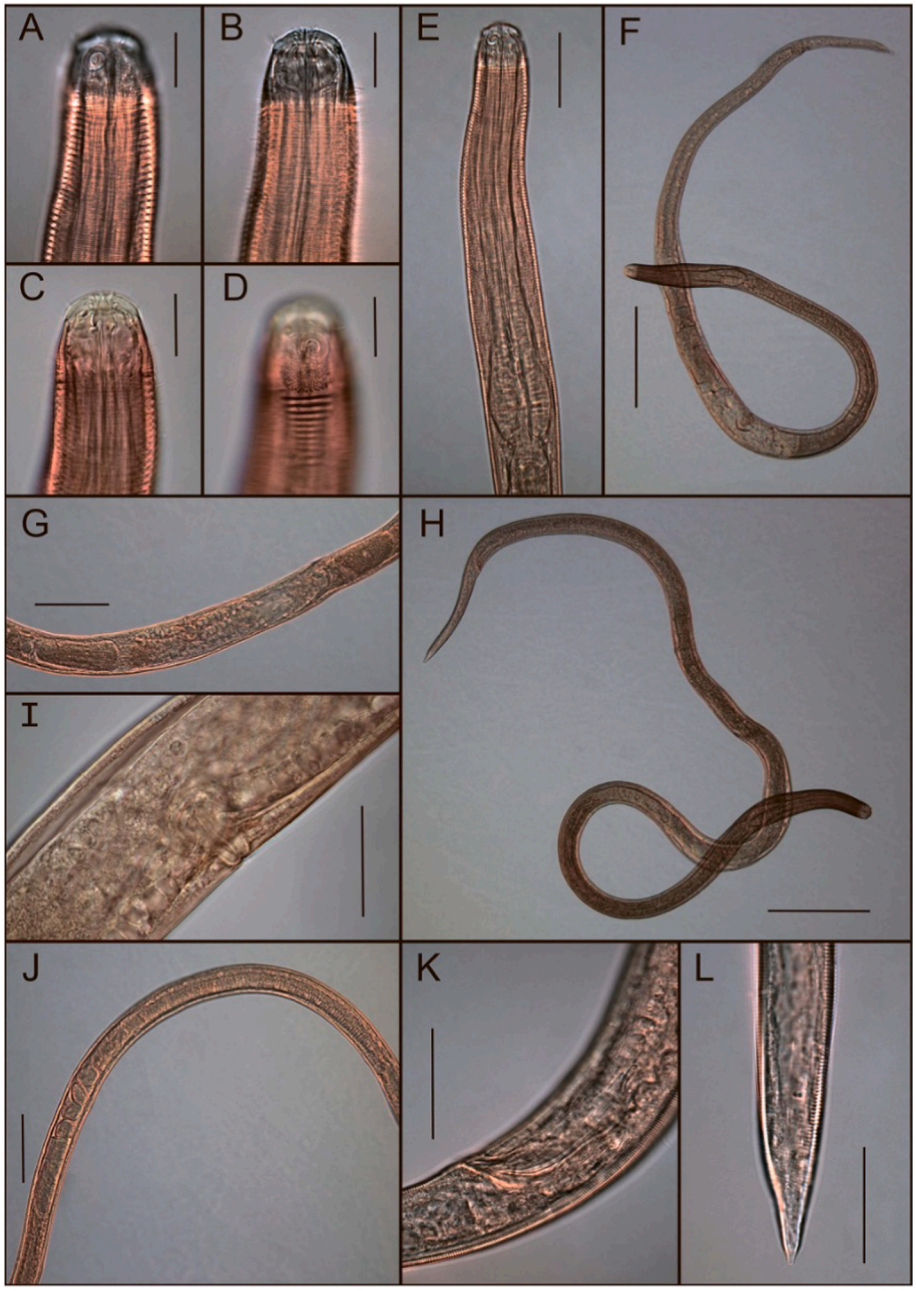

Fig. 15. *Desmodora spongiocola* sp.nov. Light microscopy, DIC. A, B. Male cephalic region. C, D. Female cephalic region. E. Female anterior region. F. Female body. G. Female reproductive system. H. Male body. J. Testis. K. Male copulatory system. L. Tail tip. Scale bars. A, B, C, D – 20 μm; E – 50 μm; F, H – 200 μm; G, J – 100 μm; I, K – 40 μm; L – 30 μm.

increased with distance from hydrothermal vents from −44.5‰ to −19.4‰. These data indicate that this species does not have obligate relationships with chemosynthetic bacteria and that it can use other available food source. The methods we used do not allow us to unequivocally state the absence of endosymbionts. However, it can be assumed that the source of carbon for them is an organic matter derived from free-living chemosynthetic bacteria.

5. Conclusion

Our data indicate the existence of typical deep-sea hydrothermal vent nematode species. Two species have been confirmed to have an extremely wide spatial distribution, they have previously been found in other reducing habitats in the Pacific and Atlantic Oceans. Studied species are characterized by a spatial specialization, preference for subhabitats (sponges, chimneys, bottom sediments with shellfish, etc.), they consume organic matter of chemosynthetic origin and some of them are

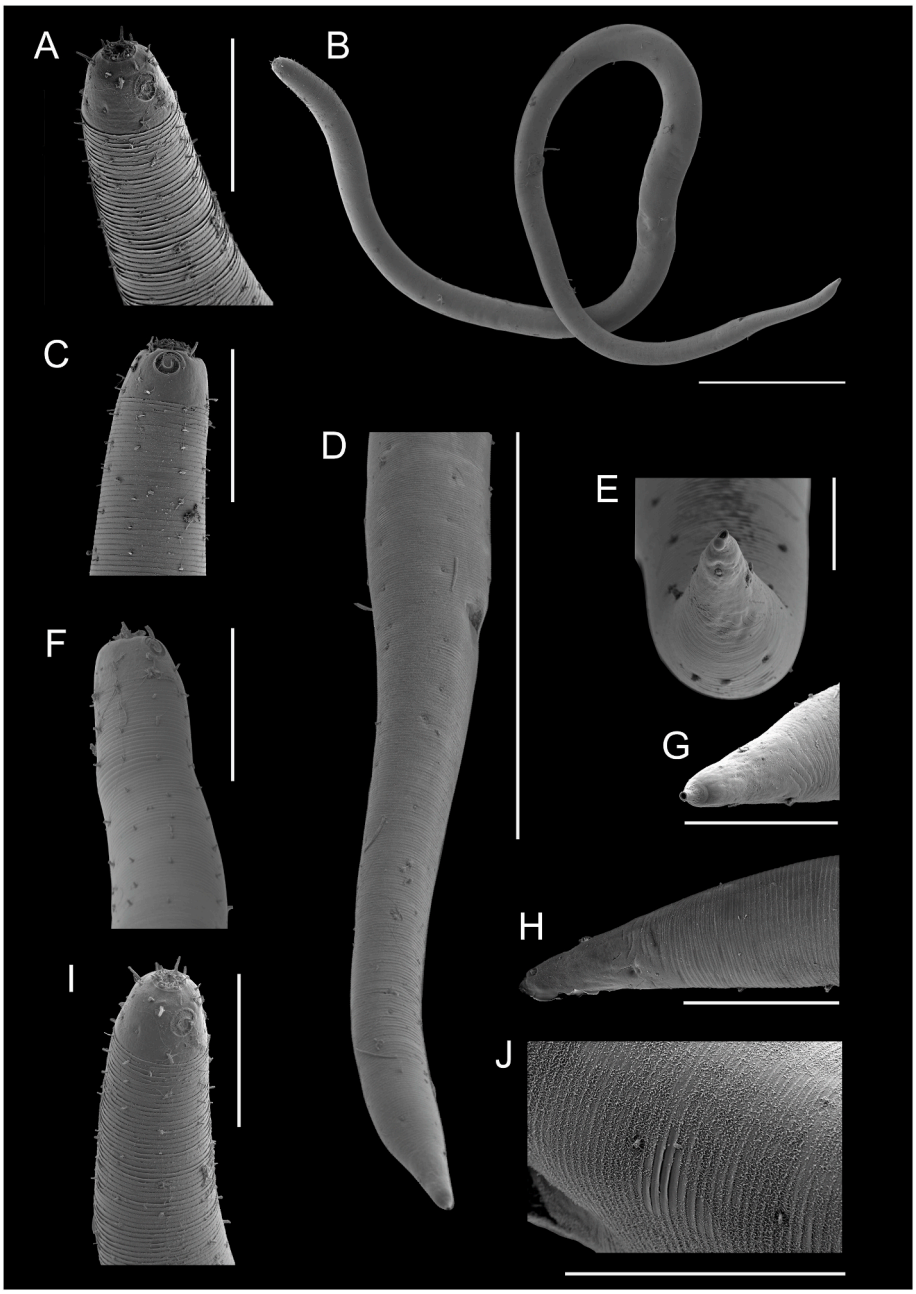

Fig. 16. *Desmodora spongiocola* sp.nov. Female. SEM. A, C, F, I. Anterior region. B. General view. D – Tail. E, G, H. Tail tip. Scale bars: A, C, F, I – 50 μm; B – 200 μm; D –100 μm; E, G, J – 10 μm; H – 20 μm.

Table 3
Interspecific p-distances (%) between the obtained sequences. Distances for 18S and 28S are under and above the diagonal respectively.

Species	*D. marci*	*D. spongiophila* sp.nov.	*D. hydrothermica* sp.nov.	*D. spongiocola* sp.nov.
D. marci		20.3 ± 1.4	14.7 ± 1.3	17.6 ± 1.5
D. spongiophila sp.nov.	7.5 ± 0.7		20.5 ± 1.6	20.7 ± 1.6
D. hydrothermica sp.nov.	5.6 ± 0.6	9.0 ± 0.6		17.1 ± 1.4
D. spongiocola sp.nov.	5.3 ± 0.6	7.8 ± 0.8	6.0 ± 0.6	

Table 4
Isotopic ($\delta^{15}N$, $\delta^{13}C$) composition of nematodes, SOM and microbial mat.

	Station	Number of individuals	$\delta^{15}N$, ‰	$\delta^{13}C$, ‰	C/N
D. spongiophila sp.nov.	1	19	10.7	−19.4	4.8
D. spongiophila sp.nov.	3	25	8.5	−27.1	4.8
D. spongiophila sp.nov.	3	25	8.3	−25.7	5.0
D. hydrothermica sp.nov.	5	150	5.7	−28.9	5.2
D. hydrothermica sp.nov.	5	150	6.2	−29.4	5.0
D. hydrothermica sp.nov.	5	150	5.8	−28.8	5.0
D. spongiophila sp.nov.	5	6		−34.7	
Microbial mat	5		6.1	−29.9	6.6
D. marci	6	50	3.9	−26.5	4.7
D. marci	6	50	2.5	−24.5	4.8
D. hydrothermica sp.nov.	6	33		−30.6	6.0
SOM	6		1.9	−26.4	6.9
Nematoda	7	200	12.2	−20.8	5.0
Nematoda	7	200	12.7	−20.8	4.9
Nematoda	7	200	12.3	−21.0	4.7
SOM	7		4.4	−23.3	7.2
D. spongiocola sp.nov.	8	32		−27.8	5.1
D. spongiocola sp.nov.	8	59	8.7	−28.6	5.0
D. spongiophila sp.nov.	8	27	7.7	−44.3	5.1
D. spongiophila sp.nov.	8	39	7.7	−44.5	4.8
D. hydrothermica sp.nov.	9	150	5.2	−28.6	5.0
D. hydrothermica sp.nov.	9	150	5.2	−28.2	5.0
D. hydrothermica sp.nov.	9	150	5.0	−29.0	5.0
Microbial mat	9		6.7	−33.2	6.4

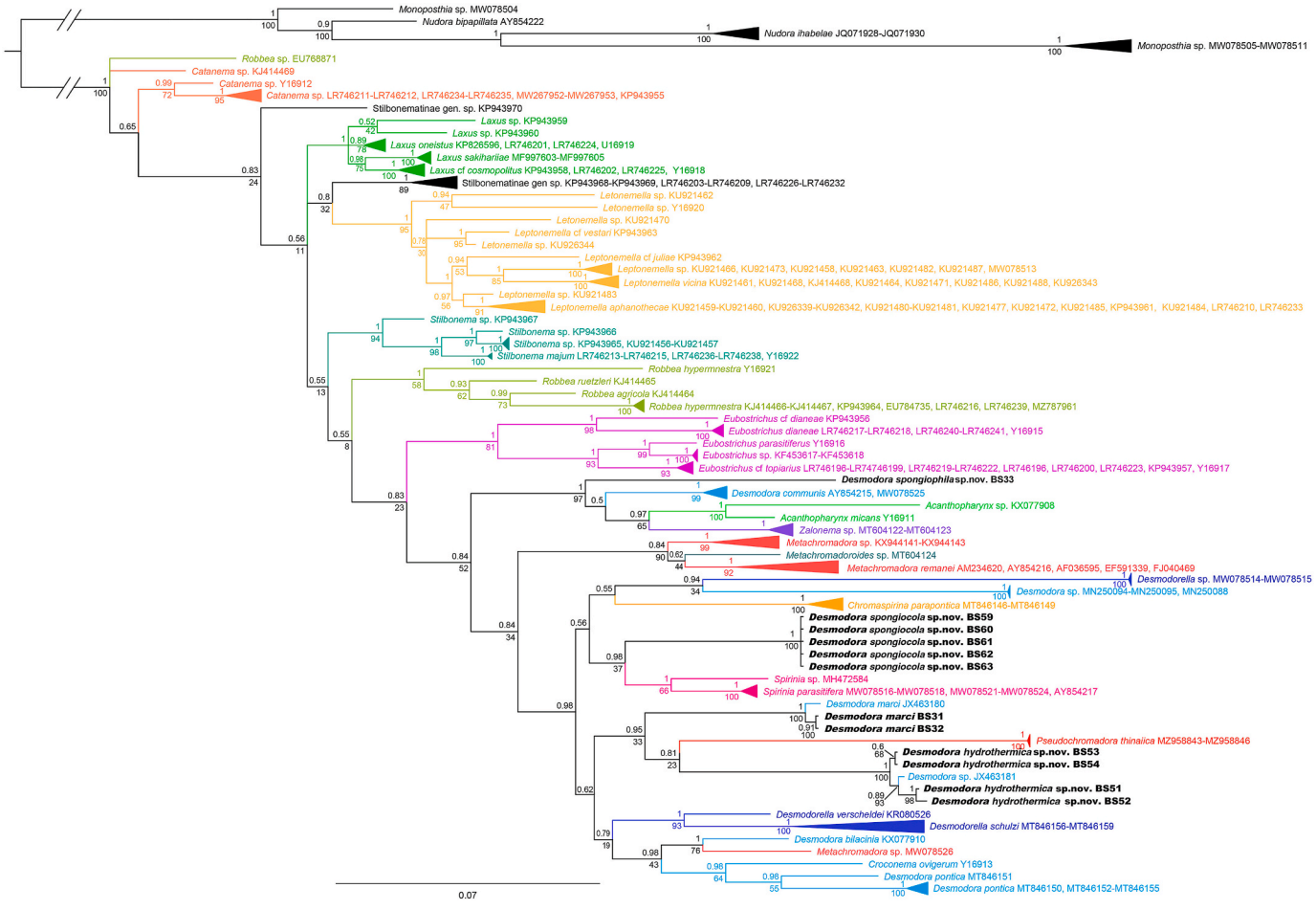

Fig. 17. Bayesian 18S rDNA phylogeny of the family Desmodoridae from 200 taxa, using the GTR + I + G model of nucleotide substitution. *Monoposthia* and *Nudora* (Monoposthiidae) were used as outgroup to root the tree. Bayesian posterior probabilities (PP) are given above tree nodes and bootstrap support values found in the ML analysis are shown below nodes.

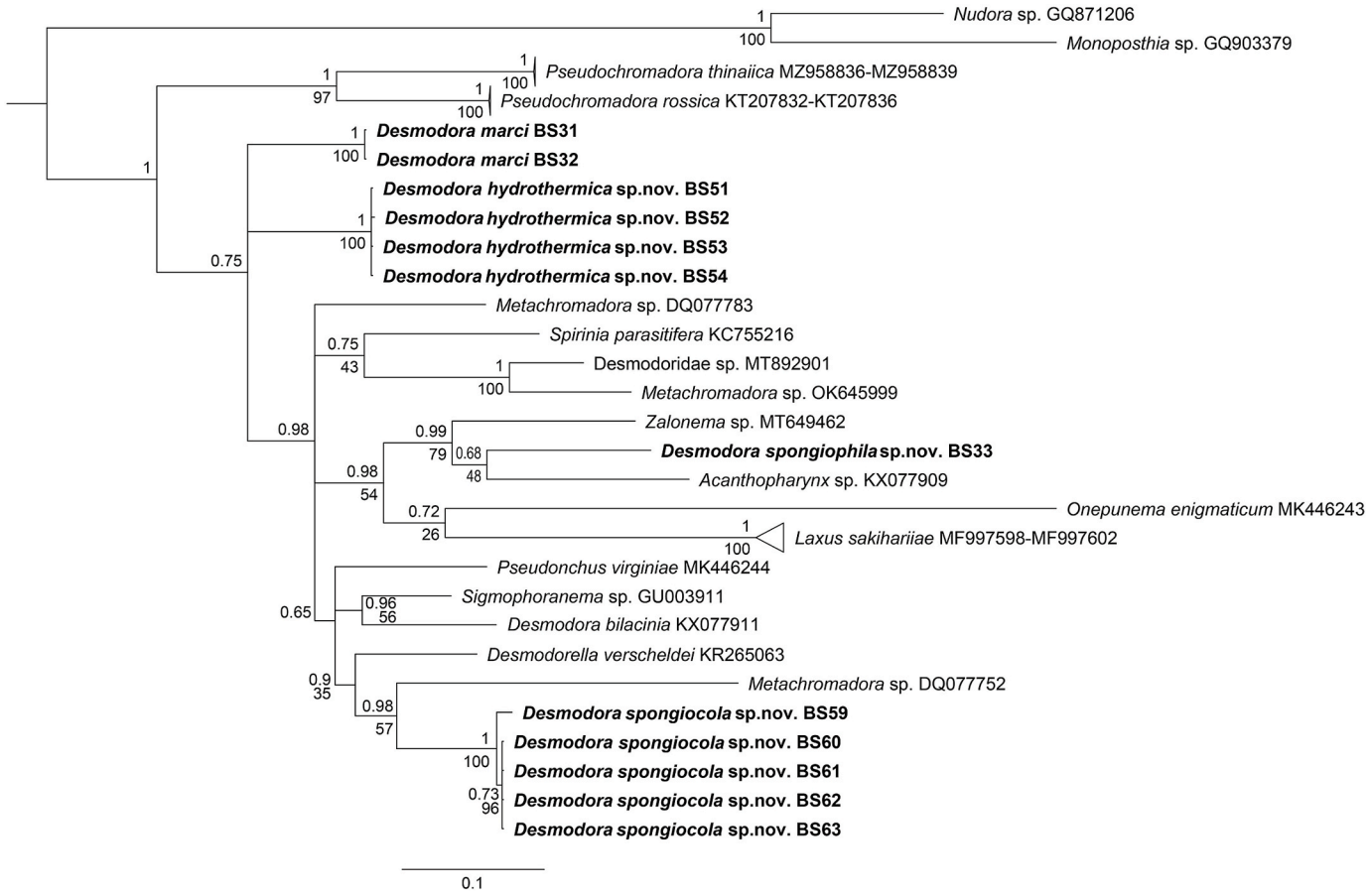

Fig. 18. Bayesian 28S rDNA phylogeny of the family Desmodoridae from 41 taxa, using the GTR + I + G model of nucleotide substitution. *Monoposthia* and *Nudora* (Monoposthiidae) were used as outgroup to root the tree. Bayesian posterior probabilities (PP) are given above tree nodes and bootstrap support values found in the ML analysis are shown below nodes.

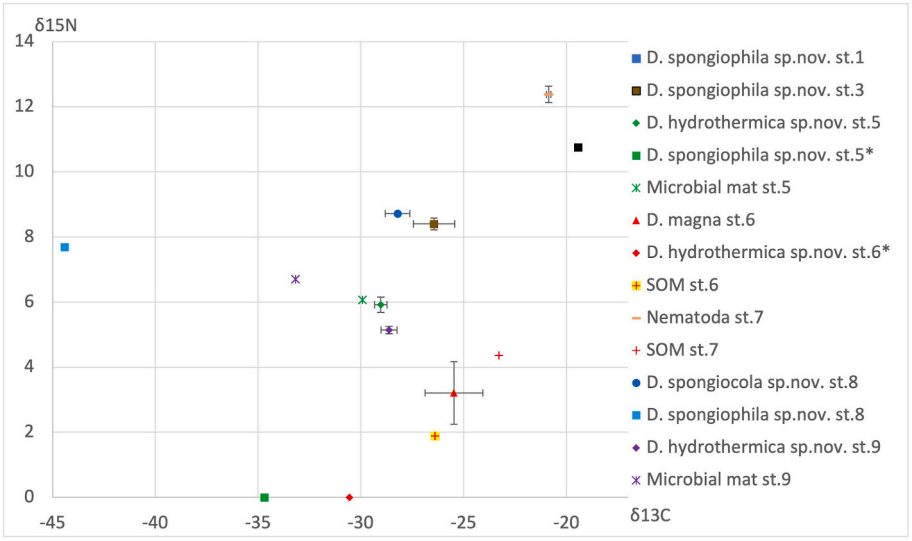

Fig. 19. Isotopic ($\delta^{15}N$, $\delta^{13}C$) composition of nematodes, SOM and microbial mat at different station (* – $\delta^{15}N$ not measured). Values are represented as mean ± standard deviation.

very abundant under extreme conditions on the surface of active hydrothermal chimneys. High abundance makes nematodes one of the most important participants in the transformation of chemosynthetically derived carbon. At the same time, some of the described species have also been found outside hydrothermal fields and they consumed photosynthetically derived carbon Thus, the question of the presence of an obligate vent nematode fauna remains open.

Table 5
Fatty acid composition (% of total, mean ± SD) of *Desmodora hydrothermica* sp. nov. (500 individuals for each replicate). The five most abundant fatty acids are shown in bold.

FA	Station 5 (n = 1)	Station 9 (n = 3)
14:1n-5	0.1	0.3 ± 0.1
14:0	1.7	1.0 ± 0.2
i15:0	0.9	0.7 ± 0.1
ai15:0	0.3	0.2 ± 0.1
15:0	0.4	0.3 ± 0.1
i16:0	0.2	0.2 ± 0.1
16:1n-7	16.9	17.8 ± 1.0
16:1n-5	0.6	0.6 ± 0.0
16:0	15.0	11.3 ± 0.6
i17:0	0.7	0.6 ± 0.0
ai17:0	0.5	0.5 ± 0.1
17:0	0.6	0.5 ± 0.0
i18:0	0.1	0.2 ± 0.1
18:2n-6	1.2	0.8 ± 0.1
18:1n-9	5.0	3.4 ± 0.1
18:1n-7	30.0	33.9 ± 0.5
18:1n-5	0.4	0.4 ± 0.1
18:0	7.0	6.1 ± 0.2
19:1n-10	0.2	0.2 ± 0.1
19:1n-8	0.2	0.2 ± 0.1
20:4n-6	0.9	0.9 ± 0.1
20:5n-3	3.3	3.5 ± 0.4
20:1n-11	1.3	1.3 ± 0.1
20:1n-9	0.6	0.5 ± 0.1
20:1n-7	2.4	3.3 ± 0.3
20:00	0.9	1.0 ± 0.1
21:1n-12	0.1	0.1 ± 0.1
21:00	0.2	0.3 ± 0.1
22:5n-6	0.2	0.3 ± 0.1
22:6n-3	1.6	1.6 ± 0.3
22:4n-6	0.1	0.2 ± 0.0
22:5n-3	0.5	0.7 ± 0.2
22:1n-7	2.3	2.9 ± 0.5
22:0	0.8	0.9 ± 0.1
24:1n-9	0.2	0.1 ± 0.1
24:1n-7	0.2	0.3 ± 0.1
24:0	0.1	0.1 ± 0.0
Unknown	2.0	2.6 ± 0.6

CRediT authorship contribution statement

V.V. Mordukhovich: Conceptualization, Data curation, Formal analysis, Methodology, Investigation, Validation, Visualization, Funding acquisition, Project administration, Writing – original draft. **N.P. Fadeeva:** Conceptualization, Formal analysis, Methodology, Investigation, Validation, Visualization, Writing – original draft. **A.A. Semenchenko:** Investigation, Visualization, Writing – review & editing. **S.I. Kiyashko:** Investigation, Writing – review & editing. **E.R. Scripova:** Investigation, Visualization, Writing – review & editing.

Declaration of competing interest

The authors declare that they have no known competing financial interests or personal relationships that could have appeared to influence the work reported in this paper.

Data availability

No data was used for the research described in the article.

Acknowledgements

The scanning electron microscopy investigations were done in the A. V. Zhirmunsky National Scientific Centre of Marine Biology FEB RAS. The authors are grateful to D.V. Fomin and A.S. Maiorova for assistance with the SEM facilities. The light microscopy investigations were done in the Laboratory of Ecology and Evolutionary Biology of Aquatic Organisms of the Far Eastern Federal University.

Fatty acid analysis was performed by V.I. Kharlamenko (1950–2019). The study would not have been possible without his help, advice, and active participation.

We thank the crews of the RV Akademik M.A. Lavrentyev for their help on board and technicians for their assistance during expeditions.

The research was supported by the grant from the Russian Foundation for Basic Research no. 20-04-00919_A.

Appendix A. Supplementary data

Supplementary data to this article can be found online at https://doi.org/10.1016/j.dsr2.2023.105267.

References

Armenteros, M., Rojas-Corzo, A., Ruiz-Abierno, A., Derycke, S., Backeljau, T., Decraemer, W., 2014a. Systematics and DNA barcoding of free-living marine nematodes with emphasis on tropical desmodorids using nuclear SSU rDNA and mitochondrial COI sequences. Nematology 16, 979–989. https://doi.org/10.1163/15685411-00002824.

Armenteros, M., Ruiz-Abierno, A., Decraemer, W., 2014b. Revision of Desmodorinae and spiriniinae (Nematoda: Desmodoridae) with redescription of eight known species. Eur. J. Taxon. 1–32. https://doi.org/10.5852/ejt.2014.96.

Baranov, B.V., Seliverstov, N.I., Murav'ev, A.V., Muzurov, E.L., 1991. The Komandorsky Basin as a product of spreading behind a transform plate boundary. Tectonophysics 199, 237–269.

Baranov, B.V., Werner, R., Rashidov, V.A., Tsukanov, N.V., Dozorova, K.A., 2021. Morphology of the Piip submarine Volcano in the Komandorsky Basin based on multibeam echosounder data. Bull. KRAESC. Environ. Sci. 2 (50), 6–21 (In Russian).

Blaxter, M.L., De Ley, P., Garey, J.R., Liu, L.X., Scheldeman, P., Vierstraete, A., Vanfleteren, J.R., Mackey, L.Y., Dorris, M., Frisse, L.M., Vida, J.T., Thomas, W.K., 1998. A molecular evolutionary framework for the phylum Nematoda. Nature 392, 71–75.

Bligh, E.G., Dyer, W.J., 1959. A rapid method of total lipid extraction and purification. Can. J. Biochem. Physiol. 37, 911–917.

Boucher, G., 1975. Nématodes des sables fins infralittoraux de la Pierre Noire (Manche occidentale). I. Desmodoridae. Bulletin du Muséum national d'Histoire naturelle, 3e série Zoologie 285, 101–128.

Bütschli, O., 1874. Zur Kenntnis der freilebenden Nematoden, insbesondere der des Kieler Hafens, vol. IX. Abhandlungen der Senckenbergischen Naturforschenden Gesellschaft, pp. 1–56.

Carreau, J.P., Dubacq, J.P., 1978. Adaptation of macro-scale method to the micro-scale for fatty acid methyl transesterification of biological lipid extracts. J. Chromatogr. A 151, 384–390. https://doi.org/10.1016/S0021-9673(00)88356-9.

Copley, J.T.P., Flint, H.C., Ferrero, T.J., Van Dover, C.L., 2007. Diversity of meiofauna and free-living nematodes in hydrothermal vent mussel beds on the northern and southern East Pacific Rise. J. Mar. Biol. Assoc. U. K. 87, 1141–1152.

Danovaro, R., Corinaldesi, C., Dell'Anno, A., Snelgrove, P.V.R., 2017. The deep-sea under global change. Curr. Biol. 27, R461–R465. https://doi.org/10.1016/j.cub.2017.02.046.

De Grisse, A.T., 1969. Redescription ou modifications de quelques techniques utilisées dans l' étude des nematodes phytoparasitaires. Mededelingen Rijksfakultiet Landbouwwetenschappen Gent 34, 352–369.

de Man, J.G., 1889. Espèces et genres nouveaux de Nématodes libres de la mer du Nord et de la Manche. Mem. Soc. Zool. Fr. 2, 1–10.

De Oliveira, D.A.S., Decraemer, W., Holovachov, O., Burr, J., De Ley, I.T., De Ley, P., Moens, T., Derycke, S., 2012. An integrative approach to characterize cryptic species in the *Thoracostoma trachygaster* Hope, 1967 complex (Nematoda: Leptosomatidae). Zool. J. Linn. Soc. 164 (1), 18–35. https://doi.org/10.1111/j.1096-3642.2011.00758.x.

Decraemer, W., Gourbault, N., 1997. Deep-sea nematodes (Nemata, Prochaetosomatinae): new taxa from hydrothermal vents and polymetallic nodule formation of the pacific (east Rise, North Fiji and Lau Basins, Clarion Clipperton fracture zone). Zool. Scripta 26 (1), 1–12.

Derycke, S., De Ley, P., De Ley, I.T., Holovachov, O., Rigaux, A., Moens, T., 2010. Linking DNA sequences to morphology: cryptic diversity and population genetic structure in the marine nematode *Thoracostoma trachygaster* (Nematoda, Leptosomatidae). Zool. Scripta 39, 276–289.

Derycke, S., Remerie, T., Vierstraete, A., Backeljau, T., Vanfleteren, J., et al., 2005. Mitochondrial DNA variation and cryptic speciation within the free-living marine nematode *Pellioditis marina*. Mar. Ecol. Prog. Ser. 300, 91–103.

Diaz-Recio Lorenzo, C., ter Bruggen, D., Luther, G.W., Gartman, A., Gollner, S., 2021. Copepod assemblages along a hydrothermal stress gradient at diffuse flow habitats within the ABE vent site (Eastern Lau Spreading Center, Southwest Pacific). Deep. Res. Part I Oceanogr. Res. Pap. 173 https://doi.org/10.1016/j.dsr.2021.103532.

Dick, G.J., Anantharaman, K., Baker, B.J., Li, M., Reed, D.C., Sheik, C.S., 2013. The microbiology of deep-sea hydrothermal vent plumes: ecological and biogeographic linkages to seafloor and water column habitats. Front. Microbiol. 4, 124. https://doi.org/10.3389/fmicb.2013.00124.

Dijkman, N.A., Kromkamp, J.C., 2006. Photosynthetic characteristics of the phytoplankton in the Scheldt estuary: community and single- cell fluorescence measurements. Eur. J. Phycol. 41, 425–434. https://doi.org/10.1080/09670260600937791.

Dinet, A., Grassle, F., Tunnicliffe, V., 1988. Premières observations sur la meiofaune des sites hydrothermaux de la dorsale Est-Pacifique (Guaymas, 21 N) et de l'Explorer Ridge. Proceedings of the hydrothermalism, biology and ecology symposium, Paris, 4–7 November 1985. Oceanol. Acta 85, 7–14.

Dodd, M.S., Papineau, D., Grenne, T., Slack, J.F., Rittner, M., Pirajno, F., O'Neil, J., Little, C.T.S., 2017. Evidence for early life in Earth's oldest hydrothermal vent precipitates. Nature 543, 60–64. https://doi.org/10.1038/nature21377.

Flint, H.C., Copley, J.T.P., Ferrero, T.J., Van Dover, C.L., 2006. Patterns of nematode diversity at hydrothermal vents on the East Pacific Rise. Cah. Biol. Mar. 47, 365–370.

Floyd, R.M., Rogers, A.D., Lambshead, P.J.D., Smith, C.R., 2005. Nematode-specific PCR primers for the 18S small subunit rRNA gene. Mol. Ecol. Notes 5 (3), 611–612. https://doi.org/10.1111/j.1471-8286.2005.01009.x.

Fry, B., 2006. Stable Isotope Ecology. Springer-Verlag, New York, p. 308.

Galkin, S.V., Ivin, V.V., 2019. Biological investigations research in Bering Sea using a remote operated vehicle Comanche. Oceanology 59, 170–172.

Galkin, S.V., Mordukhovich, V.V., Krylova, E.M., Denisov, V.A., Malyutin, A.N., Mikhailik, P., Polonik, N., Shilov, V., Ivin, V., Adrianov, A., 2019. Comprehensive research of ecosystems of hydrothermal vents and cold seeps in the Bering Sea (cruise 82 of the R/V *Akademik M.A. Lavrentyev*). Oceanology 59, 618–621. https://doi.org/10.1134/S0001437019040052.

Gerlach, S.A., 1950. Über einige Nematoden aus der Familie der Desmodoriden. Zool. Anz. 145, 178–198.

Gerlach, S.A., 1963. Freilebende Meeresnematoden von den Malediven II. Kiel. Meeresforsch. 19, 67–103.

German, C.R., Ramirez-Llodra, E., Baker, M.C., Tyler, P.A., Baco-Taylor, A., Boetius, A., Bright, M., de Siqueira, L.C., Cordes, E.E., Desbruyères, D., Dubilier, N., Fisher, C.R., Fujiwara, Y., Gaill, F., Gebruk, A., Juniper, K., Levin, L.A., Lokabharathi, P.A., Metaxas, A., Rowden, A.A., Santos, R.S., Shank, T.M., Smith, C.R., Van Dover, C.L., Young, C.M., Warén, A., 2011. Deep-water chemosynthetic ecosystem research during the census of marine life decade and beyond: a proposed deep-ocean road map. PLoS One 6. https://doi.org/10.1371/journal.pone.0023259.

Gollner, S., Govenar, B., Arbizu, P.M., Mills, S., Le Bris, N., Weinbauer, M., Shank, T.M., Bright, M., 2015a. Differences in recovery between deep-sea hydrothermal vent and vent-proximate communities after a volcanic eruption. Deep-Sea Res. Part I 106, 167–182. https://doi.org/10.1016/j.dsr.2015.10.008.

Gollner, S., Govenar, B., Fisher, C.R., Bright, M., 2015b. Size matters at deep-sea hydrothermal vents: different diversity and habitat fidelity patterns of meio- and macrofauna. Mar. Ecol. Prog. Ser. 520, 57–66. https://doi.org/10.3354/meps11078.

Gollner, S., Govenar, B., Martinez Arbizu, P., Mullineaux, L.S., Mills, S., Le Bris, N., Weinbauer, M., Shank, T.M., Bright, M., 2020. Animal community dynamics at senescent and active vents at the 9°N East Pacific Rise after a volcanic eruption. Front. Mar. Sci. 6, 832. https://doi.org/10.3389/fmars.2019.00832.

Gollner, S., Miljutina, M., Bright, M., 2013. Nematode succession at deep-sea hydrothermal vents after a recent volcanic eruption with the description of two dominant species. Org. Divers. Evol. 13, 349–371.

Hammer, Ø., Harper, D.A.T., Ryan, P.D., 2001. PAST: Paleontological statistics software package for education and data analysis. Palaeontol. Electron. 4 (1), 9pp. http://palaeo-electronica.org/2001_1/past/issue1_01.htm.

Inglis, W.G., 1968. Interstitial nematodes from St. Vincent's Bay, New Caledonia Expédition française sur les recifs coralliens de la Nouvelle Calédonie, vol. 2. Editions de la Fondation Singer-Polignac, Occasional Publications, pp. 29–74.

Jaschinski, S., Hansen, T., Sommer, U., 2008. Effects of acidification in multiple stable isotope analyses. Limnol Oceanogr. Methods 6, 12–15.

Kelly, J.R., Scheibling, R.E., 2012. Fatty acids as dietary tracers in benthic food webs. Mar. Ecol. Prog. Ser. 446, 1–22. https://doi.org/10.3354/meps09559.

Kreis, H.A., 1963. Marine Nematoda. The Zoology of Iceland 2 (14), 1–68.

Kumar, S., Stecher, G., Tamura, K., 2016. MEGA7: molecular evolutionary genetics analysis version 7.0 for bigger datasets. Mol. Biol. Evol. 33 (7), 1870–1874. https://doi.org/10.1093/molbev/msw054.

Lanfear, R., Calcott, B., Ho, S.Y., Guindon, S., 2012. Partitionfinder: combined selection of partitioning schemes and substitution models for phylogenetic analyses. Mol. Biol. Evol. 29, 1695–1701.

Leduc, D., 2021. New free-living nematode species and records (Chromadorea: Plectida and Desmodorida) from the edge and axis of kermadec trench, southwest Pacific ocean. PeerJ 9. https://doi.org/10.7717/peerj.12037.

Leduc, D., Zhao, Z.Q., 2016a. Morphological and molecular characterisation of new Acanthopharynx and Desmodora species (Nematoda: Desmodorinae) from intertidal sediments of New Zealand. Nematology 18, 905–924. https://doi.org/10.1163/15685411-00003004.

Leduc, D., Zhao, Z., 2016b. Phylogenetic relationships within the superfamily Desmodoroidea (Nematoda: Desmodorida), with descriptions of two new and one known species. Zool. J. Linn. Soc. 176, 511–536. https://doi.org/10.1111/zoj.12324.

Levin, L.A., 2005. Ecology of cold seep sediments: interactions of fauna with flow, chemistry and microbes. Oceanogr. Mar. Biol. Annu. Rev. 43, 1–46. https://doi.org/10.1201/9781420037449.ch1.

Levin, L.A., Baco, A.R., Bowden, D.A., Colaco, A., Cordes, E.E., Cunha, M.R., Demopoulos, A.W.J., Gobin, J., Grupe, B.M., Le, J., Metaxas, A., Netburn, A.N., Rouse, G.W., Thurber, A.R., Tunnicliffe, V., Van Dover, C.L., Vanreusel, A., Watling, L., 2016. Hydrothermal vents and methane seeps: rethinking the sphere of influence. Front. Mar. Sci. 3 https://doi.org/10.3389/fmars.2016.00072.

Levin, L.A., Michener, R., 2002. Isotopic evidence of chemosynthetic based nutrition of macrobenthos: the lightness of being at Pacific methane seeps. Limnol. Oceanogr. 47, 1336–1345. https://doi.org/10.4319/lo.2002.47.5.1336.

Magis, C., Taly, J.F., Bussotti, G., Chang, J.M., Di Tommaso, P., Erb, I., Espinosa-Carrasco, J., Notredame, C., 2014. T-Coffee: tree-based consistency objective function for alignment evaluation. Methods Mol. Biol. 1079, 117–129. https://doi.org/10.1007/978-1-62703-646-7_7.

Meldal, B.H.M., Debenham, N.J., De Ley, P., Tandingan De Ley, I., Vanfleteren, J.R., Vierstraete, A.R., Bert, W., Borgonie, G., Moens, T., Tyler, P., Austen, M.C., Blaxter, M., Rogers, A.D., Lambshead, P.J.D., 2007. An improved molecular phylogeny of the Nematoda with special emphasis on marine taxa. Mol. Phylogentic. Evol. 42, 622–636. https://doi.org/10.1016/j.ympev.2006.08.025.

Mordukhovich, V.V., Semenchenko, A.A., Fadeeva, N.P., Zograf, J.K., 2019. One new genus and two new free-living deep-sea nematode species with discussion of phylogeny of the family Leptosomatidae Filipjev, 1916. Prog. Oceanogr. 178, 102160 https://doi.org/10.1016/j.pocean.2019.102160.

Moura, J.D.R., Da Silva, M.C., Esteves, A.M., 2014. Four new species of *Desmodora* (Nematoda) from the deep south-east Atlantic, and a case of intersexuality in Desmodoridae. J. Mar. Biol. Assoc. U. K. 94, 85–104. https://doi.org/10.1017/S0025315413001458.

Nakasugi, F., Shimanaga, M., Nomaki, H., Watanabe, H.K., Kitahashi, T., Motomura, Y., Iseda, K., 2021. Simple harpacticoid composition observed at deep hydrothermal vent sites on sea knoll calderas in the North-west Pacific. J. Mar. Biol. Assoc. U. K. 101 (6), 947–956. https://doi.org/10.1017/S0025315421000874.

Nisbet, E., Sleep, N., 2001. The habitat and nature of early life. Nature 409, 1083–1091. https://doi.org/10.1038/35059210.

Nomaki, H., Uejima, Y., Ogawa, N.O., Yamane, M., Watanabe, H.K., Senokuchi, R., Bernhard, J.M., Kitahashi, T., Miyairi, Y., Yokoyama, Y., Ohkouchi, N., Shimanaga, M., 2019. Nutritional sources of meio- and macrofauna at hydrothermal vents and adjacent areas: Natural-abundance radiocarbon and stable isotope analyses. Mar. Ecol. Prog. Ser. 622, 49–65. https://doi.org/10.3354/meps13053.

Nunn, G.B., 1992. Nematode Molecular Evolution. Ph.D. Thesis. University of Nottingham, UK.

Pereira, T.J., Fonseca, G., Mundo-Ocampo, M., Guilherme, B.C., Rocha-Olivares, A., 2010. Diversity of free-living marine nematodes (Enoplida) from Baja California assessed by integrative taxonomy. Mar. Biol. 157, 1665–1678. https://doi.org/10.1007/s00227-010-1439-z.

Polonik, N.S., 2018. Study of gas-saturated hydrothermal fluid of the Piip submarine volcano. Processing of XXI regional scientific conference «Volcanic activity and associated processes»/Chief Editor. academician of the RAS Gordeev E.I. Petropavlovsk-Kamchatsky: IVS FEB RAS 197–199 (in Russian).

Post, D.M., 2002. Using stable isotopes to estimate trophic position: models, methods, and assumptions. Ecology 83, 703–718.

Rambaut, A., Drummond, A.J., Xie, D., Baele, G., Suchard, M.A., 2018. Posterior summarisation in Bayesian phylogenetics using Tracer 1. Syst. Biol. 7 https://doi.org/10.1093/sysbio/syy032.

Ronquist, F., Teslenko, M., van der Mark, P., Ayres, D.L., Darling, A., Höhna, S., Larget, B., Liu, L., Suchard, M.A., Huelsenbeck, J.P., 2012. Mrbayes 3.2: efficient Bayesian phylogenetic inference and model selection across a large model space. Syst. Biol. 61, 539–542.

Rybakova, E., Krylova, E., Mordukhovich, V., Galkin, S., Alalykina, I., Sanamyan, N., Nekhaev, I., Vinogradov, G., Shilov, V., Gebruk, A., Adrianov, A., 2023. Hydrothermal vent communities of the submarine Piip Volcano (the southwestern Bering Sea). Deep Sea Res. 2 Top. Stud. Oceanogr.

Sapir, A., Dillman, A.R., Connon, S.A., Grupe, B.M., Ingels, J., Mundo-Ocampo, M., Levin, L.A., Baldwin, J.G., Orphan, V.J., Sternberg, P.W., 2014. Microsporidia-nematode associations in methane seeps reveal basal fungal parasitism in the deep sea. Front. Microbiol. 5, 1–12. https://doi.org/10.3389/fmicb.2014.00043.

Seinhorst, J.W., 1959. A rapid method for the transfer of nematodes from fixative to anhydrous glycerin. Nematologica 4, 97–69.

Seliverstov, N.I., 2009. Geodynamics of the Junction Zone of the Kuril-Kamchatka and Aleutian Island Arcs. Vitus Bering of KamGU Publishing house, Petropavlovsk-Kamchatsky, p. 191 (in Russian).

Senokuchi, R., Nomaki, H., Watanabe, H.K., Kitahashi, T., Ogawa, N.O., Shimanaga, M., 2018. Chemoautotrophic food availability influences copepod assemblage composition at deep hydrothermal vent sites within sea knoll calderas in the northwestern Pacific. Mar. Ecol. Prog. Ser. 607, 37–51. https://doi.org/10.3354/meps12804.

Setoguchi, Y., Nomaki, H., Kitahashi, T., Watanabe, H., Inoue, K., Ogawa, N.O., Shimanaga, M., 2014. Nematode community composition in hydrothermal vent and adjacent non-vent fields around Myojin Knoll, a seamount on the Izu-Ogasawara Arc in the western North Pacific Ocean. Mar. Biol. 161, 1775–1785. https://doi.org/10.1007/s00227-014-2460-4.

Shirayama, Y., 1992. Studies of meiofauna collected from the Iheya Ridge during the dive 541 of the "SHINKAI 2000". Proc. JAMSTEC symp. Deep. Sea. Res. 8, 287–290.

Shirayama, Y., Ohta, S., 1990. Meiofauna in a cold-seep community off Hatsushima, central Japan. J. Oceanogr. Soc. Jpn. 46, 118–124. https://doi.org/10.1007/BF02123438.

Speth, D.R., Yu, F.B., Connon, S.A., Lim, S., Magyar, J.S., Pena-Salinas, M.E., Quake, S.R., Orphan, V.J., 2022. Microbial communities of Auka hydrothermal sediments shed light on vent biogeography and the evolutionary history of thermophily. ISME J. 16, 1750–1764. https://doi.org/10.1038/s41396-022-01222-x, 2022.

Stamatakis, A., 2006. RAxML-VI-HPC: maximum likelihood-based phylogenetic analyses with thousands of taxa and mixed models. Bioinformatics 22, 2688–2690.

Svetashev, V.I., 2011. Mild method for preparation of 4,4- dimethyloxazoline derivatives of polyunsaturated fatty acids for GC-MS. Lipids 46, 463–467. https://doi.org/10.1007/s11745-011-3550-4.

Tchesunov, A.V., 2015. Free-living nematode species (Nematoda) dwelling in hydrothermal sites of the North Mid-Atlantic Ridge. Helgol. Mar. Res. 69, 343–384. https://doi.org/10.1007/s10152-015-0443-6.

Teske, A., 2010. Sulfate-reducing and methanogenic hydrocarbon-oxidizing microbial communities in the marine environment. In: Timmis, K.N. (Ed.), Handbook of Hydrocarbon and Lipid Microbiology. Springer, Berlin, Heidelberg, pp. 2203–2223. https://doi.org/10.1007/978-3-540-77587-4_160.

Uejima, Y., Nomaki, H., Senokuchi, R., Setoguchi, Y., Kitahashi, T., Watanabe, H.K., Shimanaga, M., 2017. Meiofaunal communities in hydrothermal vent and proximate non-vent habitats around neighboring seamounts on the Izu-Ogasawara Arc, western North Pacific Ocean. Mar. Biol. 164, 1–12. https://doi.org/10.1007/s00227-017-3218-6.

Van Campenhout, J., Vanreusel, A., 2016. Closely related intertidal and deep-sea *Halomonhystera* species have distinct fatty acid compositions. Helgol. Mar. Res. 70, 1–13. https://doi.org/10.1186/s10152-016-0467-6.

Van Gaever, S., Moodley, L., Pasotti, F., Houtekamer, M., Middelburg, J.J., Danovaro, R., Vanreusel, A., 2009. Trophic specialisation of metazoan meiofauna at the Håkon Mosby Mud Volcano: fatty acid biomarker isotope evidence. Mar. Biol. 156, 1289–1296. https://doi.org/10.1007/s00227-009-1170-9.

Vanreusel, A., De Groote, A., Gollner, S., Bright, M., 2010. Ecology and biogeography of free-living nematodes associated with chemosynthetic environments in the deep sea: a review. PLoS One 5 (8), e12449. https://doi.org/10.1371/journal.pone.0012449.

Verschelde, D., Gourbault, N., Vincx, M., 1998. Revision of *Desmodora* with descriptions of new desmodorids (Nematoda) from hydrothermal vents of the Pacific. J. Mar. Biol. Assoc. U. K. 78, 75–112.

Vincx, M., Gourbault, N., 1989. Desmodoridae from the Bay of morlaix (Brittany) and the southern Bight of the North sea. Cahiers de Biologie marine. Station Biologique de Roscoff 30 (1), 103–110.

Volkman, J.K., 2006. Lipid biomarkers for marine organic matter. In: Volkman, J.K. (Ed.), The Handbook of Environmental Chemistry, vol. 2. Springer, Heidelberg, pp. 27–70.

Wada, E., Kabaya, Y., Kurihara, Y., 1993. Stable isotopic structure of aquatic ecosystems. J. Biosci. 18, 483–499.

Watanabe, H.K., Senokuchi, R., Nomaki, H., Kitahashi, T., Uyeno, D., Shimanaga, M., 2021. Distribution and genetic divergence of deep-sea hydrothermal vent Copepods (dirivultidae: siphonostomatoida: Copepoda) in the northwestern pacific. Zool. Sci. (Tokyo) 38, 223–230. https://doi.org/10.2108/zs200153.

Wieser, W., 1954. Free-living marine nematodes II. Chromadoroidea. Acta Universitatis Lundensis (NF 2) 50 (16), 1–148.

Zekely, J., Gollner, S., Van Dover, C.L., Govenar, B., Le Bris, N., Nemeschkal, H.L., Bright, M., 2006a. Nematode communities associated with tubeworm and mussel aggregations on the East Pacific Rise. Cah. Biol. Mar. 47, 477–482.

Zekely, J., Sørensen, M., Bright, M., 2006b. Three new nematode species (Monhysteridae) from deep-sea hydrothermal vents. Meiofauna Marina 15, 25–42.

Zekely, J., Van Dover, C.L., Nemeschkal, H.L., Bright, M., 2006c. Hydrothermal vent meiobenthos associated with mytilid mussel aggregations from the Mid-Atlantic Ridge and East Pacific Rise. Deep Sea Res. I. 53, 1363–1378.

Zeppilli, D., Leduc, D., 2018. Biodiversity and ecology of meiofauna in extreme and changing environments. Mar. Biodivers. 48, 1–4. https://doi.org/10.1007/s12526-017-0840-y.

Zimmermann, L., Stephens, A., Nam, S.Z., Rau, D., Kübler, J., Lozajic, M., Gabler, F., Söding, J., Lupas, A.N., Alva, V., 2018. A Completely reimplemented MPI Bioinformatics Toolkit with a new HHpred server at its Core. J. Mol. Biol. 430 (15), 2237–2243. https://doi.org/10.1016/j.jmb.2017.12.007, 2018.

Zograf, J.K., Skripova, E.R., Semenchenko, A.A., Vu, V.D., Nguyen, T.L., Phan, T.H., Mordukhovich, V.V., 2021. A novel free-living marine nematode species *Pseudochromadora thinaiica* sp. n. (Nematoda: Desmodoridae) from the seagrass bed of Vietnam. Russ. J. Nematol. 29, 169–182. https://doi.org/10.24412/0869-6918-2021-2-169-182.